Electrostatics and electrophoresis of engineered nanoparticles and particulate environmental contaminants : beyond zeta potential-based formulation

Partha Gopmandal, Jérôme F.L. Duval

Electrostatics and electrophoresis of engineered nanoparticles and particulate environmental contaminants : beyond zeta potential-based formulation.

Partha P. Gopmandal,[a] Jérôme F. L. Duval,[b *]

[a] Department of Mathematics, National Institute of Technology Durgapur, Durgapur-713209, India.

[b] Université de Lorraine, CNRS, Laboratoire Interdisciplinaire des Environnements Continentaux (LIEC), UMR 7360 CNRS-Université de Lorraine, Vandoeuvre-lès-Nancy F-54501, France.

[*]Corresponding Author: Jérôme F. L. Duval. Email: jerome.duval@univ-lorraine.fr

ABSTRACT

Colloidal nano/micro-(bio)particles carry an electrostatic charge in aqueous media and this charge is critical in defining their stability or (bio)adhesion properties, or their toxicity towards humans and aquatic biota. Determination of interfacial electrostatics of these particles is generally performed from zeta potential estimation using historical electrophoresis theory by Smoluchowski. The latter, however, strictly applies to the ideal case of hard particles defined by a surface charge distribution under the strict conditions of particle impermeability to background electrolyte ions and to (electroosmotic) flow. Herein, we review sound theoretical alternatives for capturing the electrokinetic and therewith electrostatic features of soft colloids of practical interest defined by a 3D distribution of their structural charges, and by a finite permeability to ions and/or flow (e.g. bacteria, viruses, nanoplastics, (bio)functionalized particles or engineered nanoparticles). Reasons for the inadequacy of commonly adopted hard particle electrophoresis models applied to soft particulate materials are motivated, and analytical expressions that properly capture their electrophoretic response are comprehensively reviewed.

Contacts.

- Partha P. Gopmandal.

phone: +91-72 50 27 66 90, e-mail: partha.gopmandal@maths.nitdgp.ac.in

- Jérôme F. L. Duval

phone: +33 3 72 74 47 20, e-mail: jerome.duval@univ-lorraine.fr

Keywords. Soft and hard particles, Electrophoresis, Smoluchowski equation, Soft particle electrophoresis equations, Electrostatics, Zeta potential, Bacteria, Viruses, Nanoplastics, Engineered nanoparticles.

1. Introduction

1.1. Standard theory for DC electrophoresis of colloidal particles, and concept of zeta (ς) potential.

DC Electrophoresis refers to the motion of colloidal particles in a dispersing medium under the action of a constant (frequency-independent) applied electric field. Under stationary condition, the charged

colloids surrounded by their accompanying electric double layers (EDLs) move at constant (electrophoretic) velocity as a result of the balance between electrostatic driving force and opposing viscous drag [1]. Electrophoresis is adopted to separate macromolecules (e.g. proteins, nucleic acids) [1-3], to fabricate thin films [4-5], to sequence DNA [6-7] or even microencapsulate droplets for e-paper display application [8-9]. Electrophoresis is further routinely employed to derive quantitative information on the electrostatic properties of colloidal (nano)particles (NPs) and, therewith, infer key information on e.g. their stability against aggregation [2,10]. Pending proper interpretation of electrophoretic data, measured electrophoretic mobility of colloidal particles (defined as the particle electrophoretic velocity per unit applied field strength) can be converted into an electrokinetic potential, more usually referred to as zeta (ς) potential [1,10]. The ς -potential is defined as the potential at the slip plane that separates the immobile fluid in the vicinity of the particles (the so-called stagnant layer) from the mobile fluid phase under electrophoresis measuring conditions. This potential is commonly viewed as an indicator of the density of the charges carried by the particle surface, and we refer the reader to [10] for detailed descriptions of the quantitative connections between ς -potential, surface charge density and charge density pertaining to the EDL diffuse component within classical Stern-Gouy-Chapman representations of colloidal interfaces. The reader is further referred to Delgado et al. [11] for important discussion on the contribution of the stagnant layer to particle surface conductance and its implications in terms of interpretation of electrokinetic data and ζ-potential. With respect to aspects connected to (measurable) surface conductivity of soft interfaces that are of interest in this review, readers are referred to e.g. Zimmermann et al. [12].

In literature, electrophoretic mobility values and corresponding ς -potentials can be found for numerous colloidal systems, including environmental nanoparticles like humic and fulvic acids [13-15], bacteria [16], viruses [17], engineered core-shell nanoparticles [18], aquatic contaminants like nanoplastics [19], or bio-inspired particulate systems [20]. ς -potentials have even been reported to be an adequate proxy for classifying NPs according to their respective toxicity towards microorganisms or biological tissues [21], thereby underlying the role played by electrostatics on the interactions between charged NPs and biological targets. As mentioned earlier, the ς -potential of a given colloidal particle does *not* correspond to a measured quantity but, instead, it is estimated from electrophoretic mobility data using theoretical expressions that largely differ with respect to their treatment of interfacial electrostatics and hydrodynamics [1,2,10]. Validities of these expressions are necessarily tied to some approximations, mainly with respect to the magnitude of the particle charge and/or to how the particle size compares with the Debye layer thickness, which leads to differentiation between thin and thick electric double layer regimes. Strikingly, studies reporting ς -potential values often lack a critical discussion on the choice of the theories adopted for converting the measured electrophoretic data and the true applicability of these theories to the

(bio)colloidal systems under consideration [22]. Such a discussion is however mandatory given that ζ-potential concept and standard electrokinetic theories involving this historical parameter are actually only valid for so-called **hard colloids**, i.e. colloids that are strictly impermeable both to ions from background electrolyte and to fluid flow [1,13]. These particle impermeability conditions allow indeed an accurate and unambiguous location of the slip plane often assimilated to the very surface of the particle where charges are distributed (i.e. Stern layer contributions are ignored). Metal oxide particles (e.g. hematite) and metallic colloids (e.g. AuNPs) devoid of any surrounding polyelectrolyte-like layer are illustrative examples of such hard particles.

The relationship that is most frequently used for converting measured electrophoretic mobility, μ_E, into ζ-potential is the Smoluchowski equation [23] given by $\mu_E = \varepsilon_e \zeta / \eta$ where ε_e and η are the dielectric permittivity and the viscosity of the particle dispersing medium, respectively. Smoluchowski equation can be straightforwardly derived assuming that there is no ion-conduction behind the shear plane and that particle radius (denoted as a) is immaterial compared to the Debye layer thickness, κ^{-1}, which is certainly true for sufficiently large particles and high salt concentrations in solution in line with the condition $\kappa a >> 1$ (thin EDL regime). In the other extreme of thick EDL, i.e. $\kappa a << 1$, the relevant electrophoretic mobility expression derived by Hückel [24] differs from Smoluchowski's result by a factor 2/3 due to significant effect of the retardation force [10] acting on the particles during particle electrophoretic displacement under $\kappa a << 1$ condition. Generic formulation of μ_E versus ζ-potential was elaborated by Henry [25] for the case of weakly charged colloids, a situation that renders possible the elaboration of a tractable solution of the governing set of electrohydrodynamic equations for hard particles. Henry's result reads as $\mu_E = \frac{\varepsilon_e \zeta}{\eta} f_H(\kappa a)$, where $f_H(\kappa a)$ is the so-called Henry function which captures the contribution of the retardation force on particle electrophoresis depending on the magnitude of κa that may vary between values <<1 and >>1, i.e. without restrictions on the particle size nor on the electrolyte concentration. These historical formulations by Smoluchowski [23], Hückel [24] and Henry [25] all refer to hard (impermeable) colloidal (nano)particles featuring homogeneous distribution of electrostatic charges at their surface (2D charge distribution). Obviously, many practical colloidal systems do not meet this condition, e.g. colloids that are decorated by 3D charged (bio)polymers or biocorona in complex environmental or biological media [26], porous nanodendrimers [27], or polymeric nanoparticles featuring a 'fuzzy' or 'hairy' outer surface layer [28]. Adopting too simplistic ζ-potential-based approaches to interpret electrokinetic data collected on such complex particles may lead to erroneous assessment of their electrostatic surface properties, both with respect to magnitude and sign [27]. This is particular true for

colloidal interfaces or particles harboring a zwitterionic functionality as a result of a spatial separation of their anionic and cationic functional groups in the direction perpendicular to the particle/solution interface [27,29]. For such systems, the pH value defining zero electrophoretic mobility (commonly referred to as the isoelectric point) may even depend on the concentration of indifferent monovalent electrolyte [27,29], a finding that cannot be predicted by standard electrohydrodynamic theories for hard particles [10]. The qualification 'indifferent' for ions from background electrolyte means that these ions, in contrast to so-called charge-determining ions (like protons for oxide particles), do not modify -via e.g. specific adsorption processes- the density of (structural) charges carried by the particles. In this paper, we review sound theoretical alternatives for interpreting particle electrokinetics beyond the traditional Smoluchowski or Henry levels. We further review some literature on colloidal systems of biological and environmental relevance and argue the inapplicability or approximation of standard interpretations reported for their electrokinetic properties on the basis of theoretical framework applicable to hard particles. All in all, this review paper intends to illustrate the merits of soft surface electrokinetic theories for deciphering the electrostatic characteristics of engineered particles, environmental contaminants or even biocolloids from a proper interpretation of their electrophoretic response and full integration of their fundamental particle properties including their size, structure (core-shell), 3D charge distribution, ion and flow permeabilities or interfacial heterogeneity. This paper collects useful explicit analytical expressions defining the electrophoretic mobility of such various types of so-called soft particles (polyelectrolyte, core-shell, porous, membrane-like decorated NPs), and we show that the ideal case of hard particle electrophoresis corresponds to very specific limits of these more generic expressions.

The here-reported analytical equations thus detail how the electrophoretic mobility of soft particles of practical interest (e.g. of the core-shell type) depends on electrolyte concentration, on the density of charges distributed across the inner and/or outer components of the particles, on the dimensions of particle core and/or shell components when relevant, or on the ratio between dielectric permittivities and viscosities operational in these components. The reported expressions (and the conditions underlying their legitimate applicability) further highlight how electrophoresis is sensitive to particle and interface structures (few computational examples are provided here to illustrate this aspect), a feature that is missing from Smoluchowski-based formulation of particle electrophoretic mobility. In turn, this review is intended for specialists as well as to non-specialists in the electrokinetic field, especially environmental scientists and ecotoxicologists who face the requirement to properly characterize the interface and reactivity of particles of societal concerns because of e.g. their potential toxicity towards aquatic biota or human (e.g. coated metallic particles, nanoplastics found in rivers and oceans, or particulate pharmaceutical residues, to quote only a few). This review is thus a comprehensive summary of relevant soft particle mobility expressions

that can be used for practical purposes, while insisting on the inherent limits of the Smoluchowski expression that is strictly valid for hard particles.

1.2. Invalidity of ς -potential concept for soft (permeable) particles, and theoretical alternatives specifying the inherent connections between particle structure and particle electrophoresis.

1.2.1 Polyelectrolyte (nano)particles (soft particles devoid of inner hard core)

Nanoplastic particles have gained a considerable and recent interest by the scientific community as they constitute a serious environmental challenge to terrestrial and aquatic ecosystems. These plastic debris may indeed affect e.g. living forms in oceans and rivers via their ingestion by (micro)organisms as facilitated by their small size [30]. These nanoplastics obviously present a potential threat to health of people, all the more so as there is a concern on their roles as carriers of other contaminants like heavy metals and organic pollutants [31]. Examples of nanoplastics found in the environment include polystyrene, polyvinylchloride, polyethylene, polypropylene [32-35], inks for 3D printers [36] or manufactured cosmetic and biomedical nanomaterials [37]. Accordingly, the required assessment of the fate, behavior and toxicity of these colloidal systems in aquatic environments are tied to proper evaluation of their stability properties and physical-chemical features including electrostatic charge.

Schwaferts et al. critically reviewed methods for separating nanoplastics using various force fields of thermic, electric, centrifugal or hydrodynamic origins [38]. Ramirez et al. [39] reported the surface potential of amidine polystyrene nanoplastics using Smoluchowski formulation of particle electrophoretic mobility and the electrostatic surface properties of polystyrene nanoparticles were addressed by different authors using similar formalism [40-42]. Following such Smoluchowski equation-based strategy, Hadri et al. further estimated the surface potential of nanoplastics prepared from the degradation of various microplastics including polystyrene and polyethylene [43]. Kobayashi [44] made an extensive experimental study on polystyrene latex spheres with sulfate and sulfonate functional groups, and the obtained electrophoretic mobility results were argued to be consistent with Smoluchowski equation corrected for hydrophobicity via modulation of slip length [45]. In all these studies, electrophoretic data on polymeric nanoplastics are interpreted by theoretical expressions applicable for hard colloids with 2D surface charge distribution. Nanoplastic particles are however composed of entangled polymer chains with resulting 3D distribution of the carried functional groups. This 3D polyelectrolyte-like structure confers upon the particles a certain permeability to ions and/or electroosmotic flow, which makes their assimilation to hard particle type very crude or even inappropriate. More generally, particles featuring 3D charge distribution and harboring some permeability to ions from background electrolyte and/or to flow, are termed as **soft particles**. It is emphasized here that the qualification ‘soft’ does not refer to the mechanical rigidity of the particles but to their ion and hydrodynamic permeation features.

In addition to nanoplastics, soft (nano)particulate systems include coiled polyions, biological macromolecules, proteins, nucleic acids, DNA, all being polyelectrolytes that partially or fully dissociate in electrolyte solutions depending on solution pH, with a resulting generation of a volumic charge [46-47], in contrast to the particle surface charge involved in electrokinetic theories for hard particles. Aforementioned soft particles may be devoid of hard internal core component and are accordingly sometimes qualified as **porous particles** [1]. The electrokinetic (or electrohydrodynamic) features of these colloidal systems, as reflected by their electrophoretic mobility properties, may significantly differ from that of hard particles depending on their so-called electrostatic softness and hydrodynamic softness defined by the extents of ions and flow penetrations into the particle, respectively. Hydrodynamic softness is reflected by the Brinkmann screening length [48-49] and electrostatic softness by an ion partitioning coefficient that depends on e.g. the difference between dielectric permittivity inside the particle structure and that of the aqueous medium. It is noted that depending on hydrophobicity of- and water content in- the particle, the dielectric permittivity therein can be significantly lower than that of the aqueous medium, thereby inducing a significant ion partitioning effect [50]. Based on the Debye-Hückel assumption and ensuing linearization of Poisson-Boltzmann formulation of particle electrostatics, Hermans and Fujita [51-52] derived explicit analytical expressions for the electrophoretic mobility of soft porous spheres by adopting Brinkmann and Stokes equations [48-49] to model the electroosmotic flow field distribution within and outside the particle under electrokinetic conditions. Noda et al. [53] supported the theoretical results in [51-52] upon confrontation of theory to electrophoretic mobility measurements on poly(sodium acrylate) polyelectrolyte at high background electrolyte concentrations. Other studies reported numerical analyses of the governing set of electrohydrodynamic equations for spherical porous particles without invoking linearization of Poisson-Boltzmann equation [54-59]. The inapplicability of the zeta potential concept for soft particles stems from the impossibility to accurately define the location of a shear plane at the particle/solution interface recalling that particle permeability to fluid flow goes in pair with a spatial distribution of the electroosmotic flow field within the soft particle. Even for particles defined by insignificant permeability to flow but featuring 3D charge distribution, Smoluchowski-like formulations of electrophoretic mobility are not directly applicable as they essentially ignore the way the potential distributions inside and outside the particle (and therewith the potential at the slip plane) are affected by the volumic repartition of their structural charges [27,29].

1.2.2 Composite core-shell (nano)particles

Paradigms of soft particles also encompass composite **core-shell** (bio)colloidal systems like viruses [60-61], bacteria [62-67], organic particulate matter in aquatic ecosystems [13,65,68], (bio)functionalized nanoparticles [69-71] or composite nanoparticles designed for drug delivering purpose [72]. The

electrophoretic properties of such core-shell structured particles depends generally on the physicochemical properties of the internal core (e.g. size, volumic charge density therein if relevant) as well as those pertaining to the peripheral polyelectrolyte-like layer (PEL), including density of charges, thickness, electrostatic and hydrodynamic softnesses, not to forget the impacts of pH and salt concentration [73-78]. Theoretical expressions for the electrophoretic mobility of core-shell particles comprised of a hard core (impermeable to ions and flow) and a surrounding soft PEL were elaborated mainly by Ohshima [79-81] under various electrostatic scenario (e.g. assumption or not of Donnan potential distribution inside the shell). These expressions clearly evidence that a priori location of the slip plane at the core/shell/solution interfaces can lead to dramatic misevaluation of the particle electrophoretic mobility, thereby supporting the lack of physical meaning of surface ζ-potentials for soft particulate systems.

In addition, it is worth mentioning that an electrophoretic mobility measurement performed at a single electrolyte concentration value -as often reported in literature together with associated Smoluchowski-based evaluation of ζ-potential- cannot lead to proper estimation of soft particle electrostatic features. This statement is motivated by the multiple factors that affect soft particle mobility, e.g. electrolyte concentration, particle structure (core and shell dimensions), core and shell electrostatic and/or hydrodynamic characteristics, as evidenced by refined soft surface electrokinetic formalisms [63-70,73-81]. Instead, proper electrokinetic characterization of soft particles requires electrophoretic mobility measurement as a function of medium salinity and/or pH, which allows retrieving relevant particle charge density and hydrodynamic softness at the proper level of rigor [65-66,82].

In line with this latter remark, Ohshima mobility expressions were applied successfully to interpret the electrophoretic response of various colloidal nanoparticles, including soft cationic latexes [83], antigen and antibody carrying latex particles [84], IgG-coated polystyrene particles [85], environmental humic nanoparticles [13], bacterial microorganisms [86-89], human erythrocytes of various groups [90-91], plant proteins and polysaccharides [92], microcapsule membrane [93] or guinea-pig polymorphonuclear leucocytes [94]. In addition to Ohshima, several research groups worldwide have contributed significantly to the elaboration of theories for electrophoresis of core-shell soft particles. Among them, Hill and co-workers [95-97] studied extensively the electrophoresis of core-shell particles defined by fuzzy (hairy) surface layer with analyzing the impacts of heterogeneity in charge and monomer distributions across the peripheral polymeric surface layer. Lopez-Garcia et al. [98] further studied the effects of exponentially distributed monomers and charges across particle surface layers on resulting electrophoretic mobility of core-shell particles. Duval and Ohshima [99] introduced the concept of diffuse soft interface with implementation of distribution of charges and permeable material in the governing electrohydrodynamic equations for soft core-shell and porous particles, and they analysed how such heterogeneities impacted on particle electrophoresis response versus electrolyte concentration. Additional work by Duval and

collaborators [60-61,64-69] include confrontation between soft electrokinetic theory to experimental data on various viral particles or virus-like particles with or without internal genome, respectively, on bacterial cells differing with respect to cell surface phenotype, on ion-responsive nanoparticles, and they further reported the elaboration of electrophoresis theory for multi-layered soft interfaces, which is required for viruses, or solid particles decorated by polycationic and polyanionic polyelectrolyte multilayers prepared according to e.g. the layer-by-layer deposition method [100]. A soft-step model for the segment and charge distribution across the polymer layer was introduced by Ohshima and others [101-102] and their analysis reports closed form mobility expression under Donnan electrostatic limit applicable at sufficiently high electrolyte concentrations in the thin EDL regime. Account for the impact of nonlinear effects on soft particle electrophoresis (effects that originate from e.g. relaxation/polarization of EDL) requires numerical solving of the governing electrohydrodynamic equations [cf. e.g. 60-61,66,95-99,103-110] and it is only under specific conditions of particle size, particle charge and hydrodynamic softness that closed form expressions of core-shell particle mobility with relaxation effects included can be elaborated [111]. Finally, reported soft surface electrokinetic theories differ with respect to the implementation or not of gradient of dielectric permittivity at the core/shell/solution interfaces (dielectrics-mediated ion partitioning effects) in the governing electrostatic and hydrodynamic equations [112-116]. For further details, the reader is referred to the review by Ashrafizadeh et al. [117] on most recent developments of analytical and numerical studies in soft particle electrophoresis.

All in all, in agreement with experimental data, the major features captured by adequate theories on electrophoresis of soft porous and core-shell particles may be summarized as follows :

- the existence of a finite, non-zero plateau value asymptotically reached by particle electrophoretic mobility at sufficiently high electrolyte concentrations: this remarkable property is the direct signature of the flow permeability properties of the particle that feature 3D-distributed structural charges [65,79,95,99]. This plateau is reached under salt concentration conditions in line with a *complete* screening of particle charge and of the electrostatic potential distribution. In contrast, such conditions lead to zero electrophoretic mobility for hard particles.

- the existence of an electrokinetically-active interfacial region within the soft permeable component of the charged particles, this region being that which is effectively probed by the electroosmotic flow developed under electrophoresis condition. The thickness of that intraparticulate electrokinetically-active zone depends on electrolyte concentration and hydrodynamic softness of the particle [27]. The lower is the salt concentration, the larger the electric double layer recedes within the soft particle component and the more the electrophoretic mobility will reflect electrostatic and hydrodynamic characteristics of the *internal structure* of the particles. This property actually makes it possible to derive spatial distribution of soft material density pending proper interpretation of the measured dependence of particle mobility on

electrolyte concentration [66, Supporting Information therein]. Analogies between electrophoresis of soft particles and streaming potential/current of macroscopic soft polymeric interfaces have been further established theoretically and well supported by experiments [12,29,118].

As stated above, one of the key electrokinetic properties of soft particles is that their electrophoretic mobility is not zero under conditions where their electrostatic charge is fully screened, as demonstrated by many research groups, starting with Ohshima in the 90's. In turn, a way to 'recognize' the soft character of a given particle, regardless of its nature, shape, roughness or charge distribution, is to measure by electrophoresis its mobility as a function of salt concentration. If the mobility asymptotically tends to a non-zero plateau value at sufficiently large electrolyte concentrations (which is recognized from plot of particle electrophoretic mobility *versus* salt concentration or logarithm thereof), then the particle can be qualified as soft because this finite plateau value is the direct result of intraparticulate penetration of electroosmotic flow. As mentioned earlier in this review, there are basically two types of softnesses that can be defined for soft particles: an electrostatic softness connected to the penetration of background electrolyte ions in the charged particle body, and a hydrodynamic softness that refers to the flow permeation features of the particles. For a particle defined by a 3D distribution of structural charges, impermeable to flow but permeable to background electrolyte ions (e.g. a particle with a Donnan phase), the electrokinetic interpretative framework for hard particles (strictly defined by a 2D surface charge distribution) can be applied only for qualitative orientational purpose because the magnitude and sign of the particle surface potential (which would correspond to the zeta potential for the particle considered in this development) are inherently depending on the very electrostatic properties of the inner particulate body, a feature that is *not* accounted for in the derivation of e.g. the Smoluchowski equation. The electric double layer structure and composition of soft interfaces are indeed fundamentally different from those of hard interfaces, as illustrated by the different Poisson-Boltzmann formulations of their respective interfacial potential distributions operational over the intraparticulate *and* extraparticulate regions [116,119].

In some of the studies mentioned so far on the electrophoresis of core-shell soft particles, theoretical interpretation applies to particulate systems whose hard core component is impermeable to ions from background electrolyte and to electroosmotic flow. However, there are various examples of nanoparticles where both the core component and the peripheral shell layer consist of polyelectrolyte-like chains with different composition with a resulting core and shell components that can be prone both to fluid and ion penetration depending on their *respective* hydrodynamic and electrostatic softness. Accordingly, Maurya et al. [119] refined the standard classification of soft particles between core-shell and porous types upon definition of five different classes of *core-shell composite soft particles* denoted as **Sc-Ssl** (e.g. virus particles [60]), **SSc-Ssl** (e.g. natural rubber particles [120]), **SSc-SSsl** (dendrimer nanoparticles [27]), **hard core-Ssl** (carboxyl-modified polymer nanoparticles [28]), **hard core-SSsl** (metallic particles decorated by

a layer of flow-impermeable polyelectrolyte) nanoparticles, where the nomenclature '*c*' and '*sl*' refers to the *core* and *shell* particle compartments, respectively, and '*S*' stands for *soft* polyelectrolyte i.e. permeable to both ions and fluid flow (with finite non-zero value of the Brinkmann screening length) whereas '*SS*' refers to *semi-soft* polyelectrolyte, i.e. permeable to ions *but not* to flow (the Brinkmann screening length approaches here zero) (**Figure 1**). For all these different particle types, Maurya et al. [119] derived explicit analytical expressions for the electrophoretic mobility in the thin EDL regime operational for sufficiently large particles and/or at sufficiently high electrolyte concentrations. The mathematical formulations provided by the authors illustrate the deviations of predicted electrophoretic mobility from that estimated from standard Smoluchowski-expression depending on the electrohydrodynamic features pertaining to both the core and shell compartment of the examined particles. In a recent study, Mahapatra et al [116] further extended the results by Maurya et al. [119] on *core-shell composite soft particles* electrophoresis upon account of dielectric-mediated ion partitioning effects at the core/shell/solution interfaces. These various theoretical studies make explicit the inherent connections between particle structure and electrophoretic particle properties, connections that are essentially absent from hard particle electrokinetic models.

The above classification of core shell composite soft particles and associated electrokinetic behavior beyond the Smoluchowski level is probably a plus point for an optimized design of composite particle structures featuring versatile and tunable electrostatic properties in relation to applications e.g. for delivering drugs. Instead of using free therapeutic agents to cure various diseases like cancer or diabetes, it is indeed convenient to elaborate particulate nanocarriers capable of delivering specific drugs at targeted locations so as to enhance treatment efficacy and reduce toxicity side-effects. There is an enormous development of techniques for (bio)functionalization of nanoparticles and their use as targeted drug delivering systems (TDDS), and examples include nanocarriers of core-shell composite structure, polymeric micelles, or dendrimers [121-127].

Besides the above composite core-shell soft nanoparticles, particle nanocarriers decorated by a lipidic bilayer are a promising option for TDDS engineering as (biomimetic) membrane-coated particle surfaces may prevent the occurrence of undesired immune responses [128-130]. In addition, membrane coating can increase the circulation time of the nanocarriers inside the living body and therefore enhance their targeting efficacy [131]. There is a large body of work available in literature that details possible techniques for functionalizing composite biomimetic nanocarriers with cell membrane [128-139]. Unsurprisingly, these experimental aspects have been accompanied by theoretical modelling of the electrostatic and electrokinetic properties of cell membranes and membrane-coated particles assuming fixed immobile charges within the membrane component of the particles [140-143]. As membrane layers may contain mobile molecules (e.g. free lipid molecules, charged surfactant molecules in the form of free mobile monomers) in addition to ions from electrolyte solution, Ohshima et al. [144] studied extensively the electrostatic features of lipid

membranes with account of such mobile lipid molecules therein. Jing et al. [145] further made an extensive analysis of the electrostatics of several functionalized nanoparticles like lipid-bilayer-encapsulated nanoparticles and NP-supported lipid bilayer systems. Recently, Carpenter et al. [146] calculated the surface zeta potential of an oil-water interface carrying charges due to presence of surfactant molecules from electrophoretic mobility data using Ohshima's approximation [79] for Henry's function applicable to hard colloids. Mahapatra et al. [147] analyzed the electrophoretic behavior of core-shell composite particle comprised of a hard core coated by a cell membrane-like layer without resorting to the approximate zeta-potential concept, and they evidenced how the evaluation of the intrinsic electrostatic properties of such systems from conventional electrophoretic mobility expressions for hard colloids may lead to significant error.

In the next section, we report some of the explicit analytical and tractable expressions invoked above and derived in literature for the electrophoretic mobility of *composite core-shell soft particles*, and we further report original expression for the specific case of *polyelectrolyte particles devoid of hard core*. Mobility expressions for *cell membrane coated core-shell composite (nano)particles* are further reviewed.

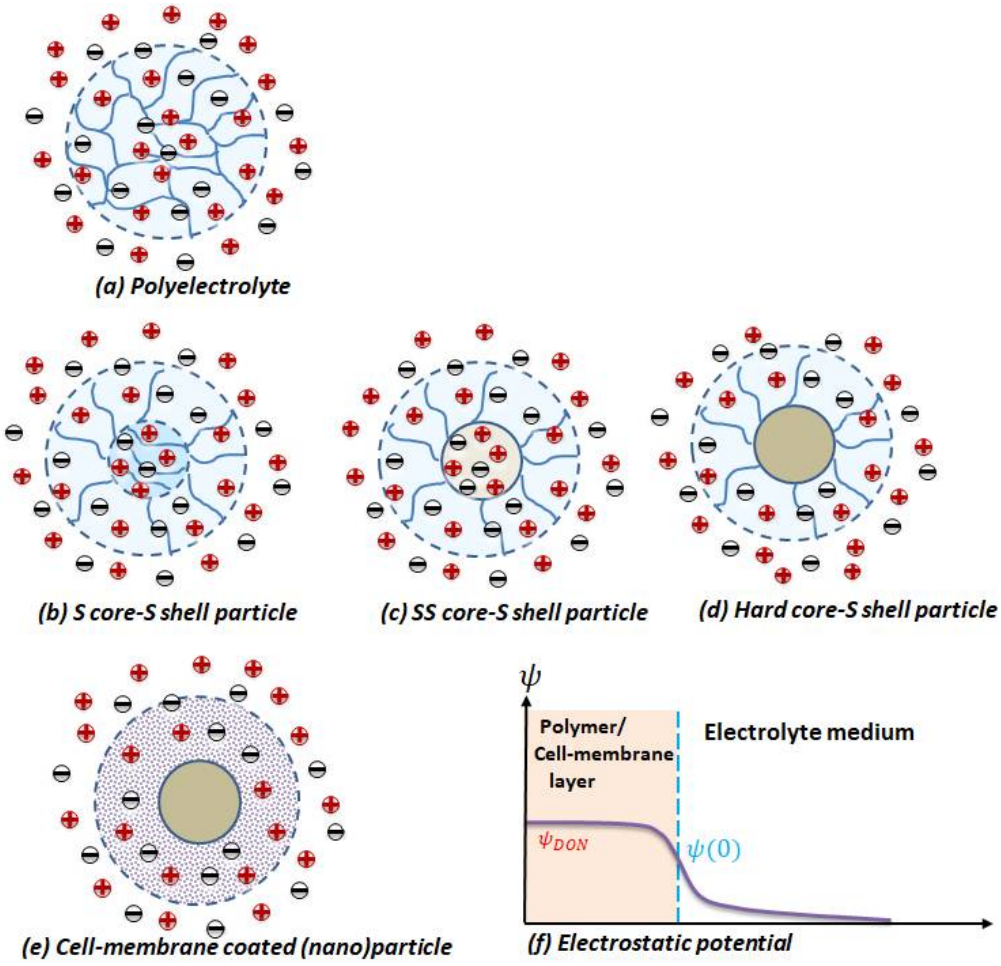

Figure 1. Schematic illustration of polyelectrolyte (nano)particles (a), various core-shell (nano)particles (Sc-Ssl, SSc-Ssl and Hard core-Ssl (nano)particles are shown in panels (b), (c) and (d), respectively) and cell membrane-like- coated (nano)particle is schemed in panel (e). '*S*' stands for *soft* polyelectrolyte particle component, i.e. permeable to both ions and fluid flow (with finite non-zero value of the Brinkmann screening length), and '*SS*' refers to *semi-soft* polyelectrolyte particle component, i.e. permeable to ions *but not* to flow (the Brinkmann screening length approaches here zero). For the sake of conciseness, the schemes pertaining to two other soft particle types (SSc-SSsl and Hard core-SSsl) [119] are not indicated. The dielectric permittivity and hydrodynamic screening length of the polyelectrolyte (nano)particle type are denoted by ε_p and λ_p^{-1}, respectively, and κ_p^{-1} defines the intraparticulate EDL thickness of such a particle. Here we use the nomenclature 'p' for polyelectrolyte. The dielectric permittivities and the hydrodynamic screening lengths pertaining to the core and shell compartments of the core-shell (nano)particle type are denoted as ε_c, ε_{sl} and λ_c^{-1}, λ_{sl}^{-1}, respectively. The EDL thicknesses κ_c^{-1} and κ_{sl}^{-1} are operational in the core and particle shell component of the core-shell (nano)particles, respectively, and the classical EDL thickness is denoted by κ^{-1}. The dielectric permittivity and viscosity of the background aqueous medium and the peripheral membrane layer of the membrane-coated (nano)particles are ε_e, η and η_m, ε_m, respectively. All in all, the nomenclature 'c' and 'sl' refers to the *core* and *shell* compartments for the core-shell (nano)particles, respectively, and 'm' refers to the membrane layer of the membrane-coated (nano)particles. In panel (f), schematic representation for the distribution of the electrostatic potential ψ in the direction perpendicular to the particle/solution interface, with the Donnan potential ψ_{DON} (potential deep inside the layer of polymer/the cell-membrane layer, strictly reached in the thin EDL limit), and with the interfacial potential denoted as $\psi(0)$. In panels (a) to (e), ions from background electrolyte are represented in the core and/or shell particle component depending on the nature of the particle considered. Everywhere in this work, volumic densities of structural charges distributed within e.g. the core and/or shell component of a core-shell particle are denoted as ρ_{core} and ρ_{shell}, quantities that should not be confused with e.g. the volumetric density of a mass.

2. Overview of analytical expressions for the electrophoretic mobility of polyelectrolyte, composite core-shell and membrane-coated nanoparticles: connecting particle structure, electrohydrodynamics and electrophoretic response.

2.1. The case of porous polyelectrolyte (nano)particles.

For the sake of demonstration and illustration, we consider here a uniform distribution of structural charges carried by a soft polyelectrolyte particle with radius b and volume charge density ρ_p (in $\mathrm{C\ m^{-3}}$).

The polyelectrolyte particle is permeable to fluid flow and the corresponding hydrodynamic Brinkmann screening length is denoted as λ_p^{-1}. The dielectric permittivities of particle and electrolyte solution are hereafter denoted as ε_p and ε_e, respectively, and the formulations thus account for dielectrics-mediated ion partitioning effects. Considering similar radius for hydrated cations and anions (r_e) in a symmetrical z:z electrolyte, the partitioning coefficient that relates to the concentrations of mobile electrolyte ions within the polyelectrolyte and in the electrolyte medium, can be written as

$$f_p = \exp\left[-\frac{(ze)^2}{8\pi r_e}\left(\frac{1}{\varepsilon_p}-\frac{1}{\varepsilon_e}\right)\frac{1}{k_B T}\right] \quad (1)$$

where k_B, T and e are Boltzmann constant, absolute temperature and elementary charge, respectively. The standard set of equations governing the electrophoresis of such polyelectrolyte particles includes the Poisson equation for the interfacial electrostatic potential distribution, the Boltzmann equation for the concentration profiles of the electrolyte ions, the conservation mass for the mobile ions and the fluid incompressibility condition. The fluid flow distribution is governed by the Darcy-Brinkman equation inside the particle whereas Stokes equation applies outside the particle in the electrolyte solution. In addition, the electrostatic potential, displacement vector, fluid velocity and shear stress are continuous across the polyelectrolyte particle/electrolyte interface. A detailed description of the corresponding governing equations describing the electrophoretic motion of polyelectrolyte particles suspended in symmetric z:z electrolyte solution of concentration n_0 (expressed in number of ionic charges per unit volume) can be found in literature, e.g. [45-54, 58-59, 78-79]. For such particles, the relevant expressions for the electrophoretic mobility μ_E derived under low to moderate charge conditions for which Debye-Hückel approximation is legitimate, are summarized in **Table 1** (Eqs. (2)-(6)). Practical limits of these expressions under various electrostatic and hydrodynamic scenario corresponding to different ratios between particle size b, Brinkman length λ_p^{-1} and Debye layer thickness κ^{-1} are detailed for particles where $\varepsilon_p/\varepsilon_e = 1$ and $\varepsilon_p/\varepsilon_e \neq 1$. The reader is further referred to the **Supporting Information** for a full demonstration of the original result (Eq. (2)) derived in this work and that we also specify in **Table 1** together with results from literature.

2.2 The case of core-shell composite (nano)particles.

In order to model electrokinetics of composite core-shell nanoparticles (particle core diameter and peripheral polymeric shell layer thickness are here denoted as L and d, respectively) in a z:z symmetrical electrolyte solution of dielectric permittivity ε_e and ionic concentration n_0, the electrostatic and hydrodynamic features of the core and shell compartments must be specified explicitly. As mentioned earlier (cf. **Figure 1**), core-shell nanoparticles can be classified according to Sc-Ssl, SSc-Ssl, SSc-SSsl,

hard core-Ssl, hard core-SSsl types depending on the extent of electrostatic softness and hydrodynamic softness of the core and shell compartments. We recall that the nomenclature '*c*' and '*sl*' refers to the *core* and *shell* compartments, respectively, '*S*' stands for *soft* polyelectrolyte component permeable to both ions and flow and '*SS*' refers to *semi-soft* polyelectrolyte component which is permeable to ions *but not* to flow. The dielectric permittivities and Brinkman screening lengths of the particle shell and particle inner core are hereafter denoted as ε_{sl}; ε_c and λ_c^{-1}; λ_{sl}^{-1} , respectively, with the inequalities of practical interest $\varepsilon_e > \varepsilon_{sl}$ and $\varepsilon_e > \varepsilon_c$ and $\lambda_c^{-1} < \lambda_{sl}^{-1}$. The difference in dielectric permittivity of electrolyte medium, core and shell compartments contributes to the partitioning of mobile electrolyte ions. The partitioning of mobile electrolyte ions between inner core and electrolyte solution, outer shell and electrolyte medium are now given by

$$f_j = \exp\left[-\frac{(ze)^2}{8\pi r_e}\left(\frac{1}{\varepsilon_j}-\frac{1}{\varepsilon_e}\right)\frac{1}{k_B T}\right] \quad , \quad j = c, sl \tag{7}$$

Like Eq. (1), Eq. (7) holds for similar radius of the electrolyte cations and anions (r_e). We further denote the densities of net amounts of charges entrapped in the inner core and in the outer shell volumes as $\rho_{core} = z_c F N_c$ and $\rho_{shell} = z_{sl} F N_{sl}$, respectively. Here z_c, z_{sl} and N_c, N_{sl} are the valences and concentrations of immobile structural charges carried by the core and by the shell particle component, respectively. A detailed description of the governing electrohydrodynamic equations and associated boundary conditions are given in literature [79-81,116,119] for core-shell particle types. **Table 2** collects the resulting mobility expressions (Eqs (8)-(22)) for Sc-Ssl (Eqs. (8)-(12)), SSc-Ssl (Eq. (13)), SSc-SSsl (Eq. (14)), hard core-Ssl (Eqs. (15)-(21)), hard core-SSsl types (Eq. (22)) in the thin EDL regime where particles curvature effects on electrostatics and hydrodynamics are negligible (so-called flat-plate representation) and with assuming low to moderate particle charge limit for which the Debye-Hückel approximation is valid. **Table 2** systematically specifies the conditions underlying the validity of the reported expressions and obviously, any application of these equations is tied to verification of these conditions. It is stressed that Ohshima developed the general form of the electrophoretic mobility of hard core-Ssl nanoparticles for poorly charged particles, albeit the derivation involves complicated definite integrals [78-81]. Most results given in **Table 2** were derived from the work by Mahapatra et al. [116] and they correctly match the expressions developed by Maurya et al. [119] in the limit $\varepsilon_e = \varepsilon_{sl} = \varepsilon_c$. Ashrafizadeh [117] made a specific review on the electrophoresis of hard core-Ssl nanoparticles and the reader is referred to that review for further details.

2.3. The case of cell membrane coated core-shell (nano)particles.

In this section, we comment on the theoretical expressions available in literature for the electrophoretic mobility of functionalized core-shell nanoparticles coated with cell-membrane. In general, the membrane of various biological cells bears mobile charges due to the presence of free lipid molecules, or charged

surfactant molecules, and this generates surface charge along the membrane-to-electrolyte interface. According to Singer and Nicolson [148], the cell-membrane consists of a lipid bilayer that can be considered as a two-dimensional oriented viscous solution. In addition, the dielectric permittivity of the membrane-coating is generally much lower than that in the aqueous medium, and therefore a significant dielectrics-mediated ion partitioning effect is expected. We denote as η_m and ε_m the viscosity and dielectric permittivity of the membrane (subscript 'm'), respectively. The particle with peripheral cell-membrane of thickness δ is immersed in a symmetric z: z electrolyte solution of bulk concentration n_0 (volume density of ions in bulk solution). The spatial distribution of electrolyte concentration of ions in solution and along the membrane-to-electrolyte interface satisfies $n_i(\delta^-) = f_m n_i(\delta^+)$, where the ion partitioning coefficient f_m (considering equal radius r_e of electrolyte cations and anions) is given here by

$$f_m = \exp\left[-\frac{(ze)^2}{8\pi r_e}\left(\frac{1}{\varepsilon_m}-\frac{1}{\varepsilon_e}\right)\frac{1}{k_B T}\right] \tag{23}$$

The density of additional free lipid molecules in the peripheral shell layer is denoted as N_0 with valence Z. Furthermore, the surface charge at the membrane/electrolyte interface must be introduced and it is denoted as σ (in C m^{-2}). Under the assumption $\kappa\delta \gg 1$, where κ^{-1} is the EDL thickness, the potential inside the cell membrane reaches Donnan potential. For membrane decorated core-shell particle, the Donnan potential ψ_{DON} deep inside the peripheral membrane coating (**Figure 1f**) is given by [147]

$$\psi_{DON} = \frac{k_B T}{ze}\left[\frac{ZN_0}{2zf_m n_0}+\sqrt{1+\left(\frac{ZN_0}{2zf_m n_0}\right)^2}\right] \tag{24}$$

and the potential along the cell membrane/electrolyte interface $\psi(0)$ (**Figure 1f**) can be obtained from the relationship [147]

$$\psi(0) = \frac{\frac{\sigma}{\varepsilon_e k}-Sgn(\psi(0))\psi_{DON}\sqrt{f_m\frac{\varepsilon_m}{\varepsilon_e}(1+Zy_{DON})}}{1-Sgn(\psi(0))\sqrt{f_m\frac{\varepsilon_m}{\varepsilon_e}(1+Zy_{DON})}} \tag{25}$$

where y_{DON} is the Donnan potential scaled by the thermal potential $k_B T/e$. As the membrane is treated as a viscous solution (Singer and Nicolson [148]), the fluid flow along the peripheral membrane and in the electrolyte solution are governed by Stokes equation upon considering differences between viscosity of the membrane (η_m) and that in bulk aqueous medium (η). The body force term operational inside the peripheral liquid layer must be further modified via consideration of the ion partitioning effects. Finally, as in previous sections, spatial profiles of mobile ion concentrations are dictated by Boltzmann equation, and the electrolyte potential distribution is governed by Poisson equation. Applying the relevant electrostatic and hydrodynamic boundary conditions at the membrane/electrolyte interface (e.g. continuity of potential, displacement vector, velocity, shear stress and Maxwell stress), the electrophoretic mobility of such particle under $\kappa\delta \gg 1$ condition takes the simple form [147]

$$\mu_E = \left(\frac{\varepsilon_e}{\eta} - \frac{\varepsilon_m}{\eta_m}\right)\psi(0) + \frac{\varepsilon_m}{\eta_m}\psi_{DON} \quad (26)$$

where $\psi(0)$ and ψ_{DON} are defined by Eqs. (25) and (24), respectively. Under the limit $\eta_m \gg \eta$, the above expression correctly reduces to the following Smoluchowski limit

$$\mu_E = \frac{\varepsilon_e \psi(0)}{\eta} \quad (27)$$

The electrophoretic mobility expressions applicable to particulate polyelectrolytes (**Table 1**), core-shell composite NPs (**Table 2**) and cell membrane-coated NPs (Eq. (26)) are all superior to the Smoluchowski formulation of hard particle electrophoresis mobility as they offer a way to account for contributions from core-shell particle structure, relevant volumic charge densities and ion/flow permeabilities. It is only under specific conditions in terms of respective magnitudes of core/shell dimensions, salt concentration and Brinkman length scale, that the defining mobility expressions of composite soft (nano)particles or membrane-coated (nano)particles adopt a structure reminiscent of that of the standard Smoluchowski equation. We report in **Table 3** all these conditions together with the corresponding Smoluchowski-like mobility expressions (Eqs. (28)-(37)) and the type of (nano)particles they apply to. It is remarkable that all these Smoluchowski-like expressions systematically involve the interfacial potential $\psi(0)$ (**Figure 1**), with the noticeable difference that -unlike in the historical Smoluchowski formulation- $\psi(0)$ is intimately connected to the structure and to the electrohydrodynamic properties of the particles as specified in **Table 3.**

3. Computational illustrations of the dependence of electrophoretic mobility on particle type.

In this section, we illustrate how the scaled electrophoretic mobility μ_E/μ_0 (with $\mu_0 = \varepsilon_e e/(\eta k_B T)$) of various NPs considered in the preceding sections (e.g., polyelectrolyte (nano)particles, core-shell composite NPs, membrane-coated NPs) are affected by salt concentration or other key variables including particle core and/or shell permeabilities to fluid flow. The underlying effects, commented in the literature, are discussed. For the examples provided below, the dielectric permittivity and viscosity of the background electrolyte solution are taken to be $\varepsilon_e = 80\,\varepsilon_0$ and $\eta = 10^{-3}$ Pa s, where ε_0 refers to the dielectric permittivity of the vacuum.

In Figure 2a we show some results for the electrophoretic mobility of polyelectrolyte NPs (Eq. (2)) as a function of dielectric permittivity ratio of polyelectrolyte to background electrolyte solution (i.e., $\varepsilon_p/\varepsilon_e$). Note that the quantity $\varepsilon_p/\varepsilon_e$ mediates the electrostatic softness of the polyelectrolyte and it can take values between 0 and 1 depending on the specific chemical composition of the polyelectrolyte. With $0 < \varepsilon_p/\varepsilon_e < 1$, an increase in $\varepsilon_p/\varepsilon_e$ increases the NP electrostatic softness and enhances the accumulation of electrolyte ions within the polyelectrolyte NPs, which in turn reduces bulk electrostatic potential and therewith particle electrophoretic mobility. In line with expectation, particle electrophoretic mobility derived from Eq. (2)

reduces to that defined by Eq. (3) for $\varepsilon_p = \varepsilon_e$. Figure 2a further illustrates that particle mobility increases with increasing κ_p^{-1} which refers to the EDL thickness inside the polyelectrolyte particle where operational dielectric permittivity is ε_p (κ_p^{-1} reduces to κ^{-1} in the limit $\varepsilon_p/\varepsilon_e = 1$). An increase in κ_p^{-1} goes in pair with a decrease in background electrolyte concentration, which leads to a decrease of the particle charge neutralization by counterions as intraparticulate accumulation of the latter decreases, so that in turn particle electrophoretic mobility increases.

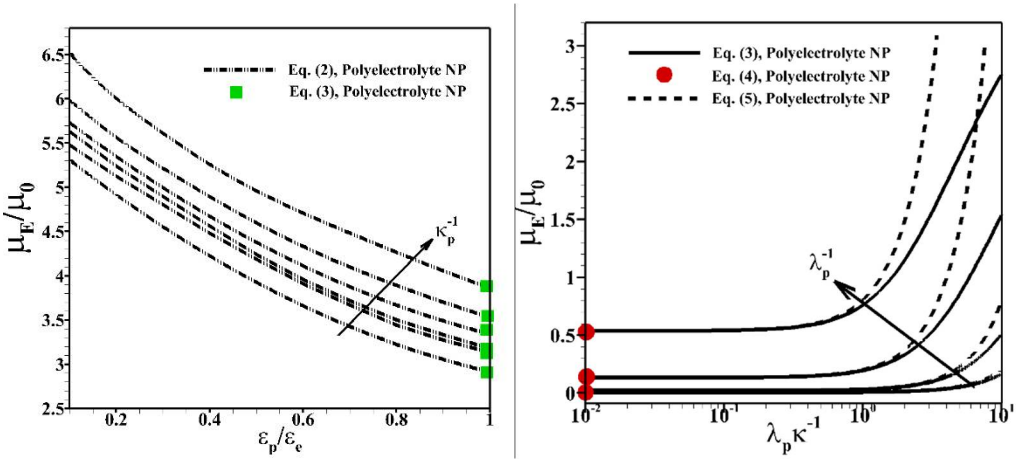

(a) (b)

Figure 2: Key variations of scaled electrophoretic mobility μ_E/μ_0 for *polyelectrolyte NPs* are shown. Results derived from Eq. (2) in (a) as a function of permittivity ratio $\varepsilon_p/\varepsilon_e$ for different κ_p^{-1} (=0.1, 1, 2, 5, 10, 20 nm) at fixed $\lambda_p^{-1} = 20$nm (lines). The direction of the arrow in (a) represents increasing values of κ_p^{-1}. Symbols in (a) correspond to predictions from Eq. (3) valid for $\varepsilon_p = \varepsilon_e$. In (b), scaled electrophoretic mobility derived from Eqs. (3) and (5) (specified) versus $\lambda_p\kappa^{-1}$ for different values of λ_p^{-1} (=1, 2, 5, 10 nm) at fixed $\varepsilon_p = \varepsilon_e$. The direction of the arrow in (b) represents increasing values of λ_p^{-1}. Symbols in (b) correspond to predictions from Eq. (4) valid in the thin EDL limit (i.e., $\kappa \to \infty$). Other model parameters: b=50 nm, $z_p = 1$ and N_p=1mM.

To illustrate the importance of the relative magnitude of EDL thickness (κ^{-1}) as compared to the hydrodynamic screening length (λ_p^{-1}) on the electrophoretic mobility of polyelectrolyte NPs, we report in Figure 2b electrophoretic mobility versus $\lambda_p\kappa^{-1}$ for various values of hydrodynamic screening length λ_p^{-1} under the condition $\varepsilon_p = \varepsilon_e$ on the basis of Eq. (3). At a given λ_p^{-1}, the particle mobility increases with increasing $\lambda_p\kappa^{-1}$, which is according to expectation as particle charge screening then reduces. As mentioned in preceding developments, a plateau value is reached by the particle electrophoretic mobility

for sufficiently thin EDL (sufficiently high salt concentration), and expression of that plateau value is given by Eq. (4) applicable when κ^{-1} goes to 0. As anticipated, with increasing λ_p^{-1} the screening of the electroosmotic flow across the polyelectrolyte NP becomes less pronounced and this is thus accompanied by an increase in electrophoretic mobility. It is noted that the simplified mobility expression given by Eq. (5) valid under the inequalities conditions $\kappa b \gg 1$ and $\lambda_p\, b \gg 1$ systematically overestimates particle mobility predictions from Eq. (3) in the regime corresponding to $\lambda_p \kappa^{-1} > 1$. In this regime, the approximations underlying the applicability of Eq. (5) for the example treated in Figure 2b are indeed not verified.

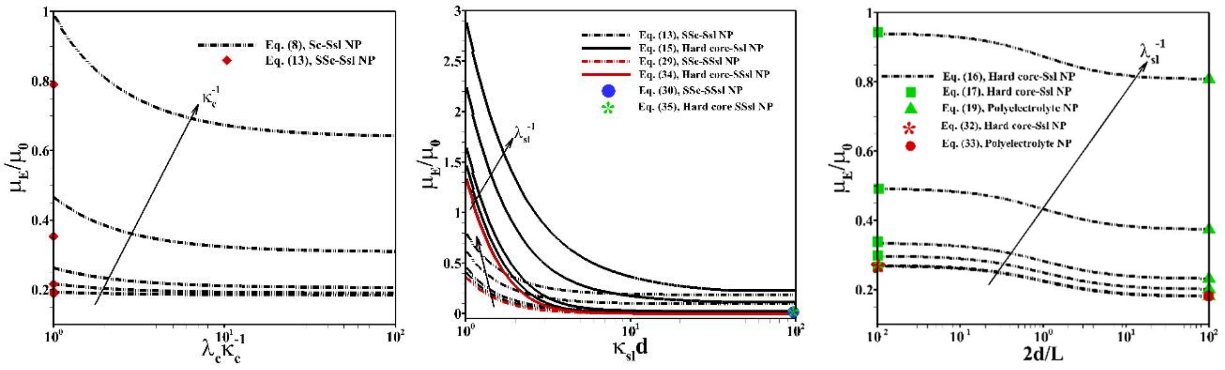

(a) (b) (c)

Figure 3: Variations of scaled electrophoretic mobility μ_E/μ_0 for various *core-shell composite NPs* are shown. Results are given in (a) for Sc-Ssl particle (Eq. (8)) as a function of $\lambda_c \kappa_c^{-1}$ for different values of κ_c^{-1} (=0.1, 1, 2, 5, 10 nm) at fixed $\lambda_{sl} d$ $(= 1)$. The direction of the arrow in (a) represents increasing values of κ_c^{-1}. In (a) we have further indicated results valid for SSc-Ssl NPs (Eq. (13)). In panel (b), results are provided for SSc-Ssl NPs (Eq. (13)) and hard core-Ssl NPs (Eq. (15)) as a function of $\kappa_{sl} d$ for different values of λ_{sl}^{-1}(= 0.01, 0.1, 1, 5, 10 nm). The direction of the arrow in (b) represents increasing values of λ_{sl}^{-1}. Predictions for SSc-SSsl NPs (Eq. (29)) and hard core-SSsl NPs (Eq. (34)) are also included in panel (b). For comparison purpose, we have further reported data from Smoluchowski-like mobility expressions given by Eqs. (30) and (35). Other model parameters in panels (a) and (b): $z_c = 1$, $z_{sl} = 1$, N_c =1 mM, N_{sl} =1mM, $\varepsilon_c = 0.5\, \varepsilon_e$, $\varepsilon_{sl} = 0.75\, \varepsilon_e$, d=10 nm, L = 100 nm. In panel (c), results are given for hard-core Ssl NPs (Eq. (16)) as a function of the ratio $2d/L$ between thickness of the peripheral soft layer and particle inner core radius at fixed d=100 nm and $\kappa_{sl}^{-1} = 1$ nm. The results are given for different values of λ_{sl}^{-1} (= 0.01, 0.1, 1, 5, 10 nm) and direction of the arrow represents increasing values of λ_{sl}^{-1}. We have further reported the electrophoretic mobility results for the limiting cases defined by Eqs. (17), (19), (32) and (33). Here κ_c^{-1} and κ_{sl}^{-1} stand for the EDL thicknesses operational in the core and particle shell component where operational dielectric permittivities are ε_c and ε_{sl}, respectively.

In Figure 3a, the impact of hydrodynamic screening length (λ_c^{-1}) in the particle core-compartment of Sc-Ssl NPs on the electrophoretic mobility (Eq. (8)) is shown for different EDL thickness κ_c^{-1} (=0.1, 1, 2, 5, 10 nm) at fixed $\lambda_{sl}d$ (= 1). Readers are referred to the figure caption for specification of other adopted model parameters. At given κ_c^{-1}, particle mobility reduces with increasing $\lambda_c\kappa_c^{-1}$and reaches a non-zero plateau value at sufficiently small hydrodynamic screening lengths (i.e., large $\lambda_c\kappa_c^{-1}$). With increasing $\lambda_c\kappa_c^{-1}$ at fixed κ_c^{-1}, the screening of the electroosmotic flow (EOF) inside the inner particle compartment increases, which leads to an increment of counterion accumulation across the inner compartment. As a result, particle mobility reduces with increasing $\lambda_c\kappa_c^{-1}$ at fixed κ_c^{-1}. At fixed λ_c^{-1}, particle mobility increases with EDL thickness κ_c^{-1} for reasons already invoked in Figure 2. The particle mobility achieved in the thin EDL regime is again non-zero, which is -as previously discussed- an intrinsic property of core-shell composite NPs. In Figure 3a, we have further reported results derived from Eq. (13) for SSc-Ssl NPs (where inner core allows penetration of ions but not fluid flow) to make a quantitative comparison between electrophoresis of Sc-Ssl and SSc-Ssl NPs. We observed that electrophoretic mobility of SSc-Ssl NP is smaller (in magnitude) than that of Sc-Ssl NP, especially in the thick EDL regime (large κ_c^{-1}). In this regime, screening of EOF across the core compartment of the Sc-Ssl NPs is indeed less significant, and the electrokinetically-active particle region is thus more extended than that for SSc-Ssl NPs type. At sufficiently small κ_c^{-1} (thin EDL regime), the screening of EOF across the core compartment is largest, which leads to similar mobility of Sc-Ssl NPs and SSc-Ssl NPs under such conditions.

In Figure 3b, results are given for SSc-Ssl (Eq. (13)) and hard core-Ssl (Eq. (15)) NPs as a function of electrolyte concentration at fixed shell layer thickness (d = 10 nm). Data are presented for various values of the hydrodynamic screening length of the shell compartment. For the sake of comparison, results pertaining to SSc-SSsl (where both inner core and shell are permeable to ions but not fluid flow) are also included (Eqs. (29)) together with those for hard core-SSsl NPs (where shell is permeable to ions but not to fluid flow) (Eq. (34)). At sufficiently small hydrodynamic penetration lengths, mobilities of SSc-Ssl and hard core-Ssl particles correctly merge with those of SSc-SSsl and hard core-SSsl particles, respectively. In addition, we observe that the mobility of hard core-Ssl NPs is higher compared to that of SSc-Ssl NPs. Indeed, SSc-Ssl NPs allowing penetration of mobile electrolyte ions in their core compartment, their interfacial electrostatic potential is reduced (larger screening of the particle charge) and so is their electrophoretic mobility. In line with expectation, the mobility of both SSc-Ssl and hard core-Ssl NPs decreases with decreasing EDL thickness and hydrodynamic screening length. This finding is explained by a significant screening of the EOF through the shell compartment. At sufficiently large $\kappa_{sl}d$ (with the Donnan potential limit being reached for $\kappa_{sl}d \gg 1$), the electrophoretic mobility of SSc-SSsl and hard core-SSsl NPs correctly approaches the limits given by Eqs. (30) and (35), respectively.

We have reported in Figure 3c predictions from the mobility expression Eq. (16), which applies to both hard core-Ssl and polyelectrolyte NP pending proper specification of L and d. Data are provided as a function of the shell layer thickness (d) to core radius $(L/2)$ ratio for various hydrodynamic screening lengths of the shell layer. As expected, particle mobility increases with increasing λ_{sl}^{-1}. We have further explicitly reported the limiting cases $d \ll L/2$ and $d \gg L/2$ given by Eqs. (17) and (19), which corresponds to the mobility expressions for hard core-Ssl under Donnan limit and for polyelectrolyte NPs (i.e. devoid of inner hard core), respectively. It is remarkable that results from Eqs. (17) and (19) differ by a factor $2/3$. This factor originates from the presence of the polyelectrolyte where electric field lines are significantly distorted, unlike the case of hard core-Ssl particles for which the electric field lines remain parallel to the surface of the hard inner core. In the limit $\lambda_{sl} \to \infty$ where the shell layer is impermeable to fluid flow, the mobility expressions (17) and (19) approach the results derived from simplified Smoluchowski and Hückel expressions, respectively, with an interfacial potential that is half of the Donnan potential. We finally mention that expressions (32) and (33) also differ by a factor $2/3$, whose origin is similar to that explaining why mobility expressions for hard colloids are different in the thin and thick EDL regimes.

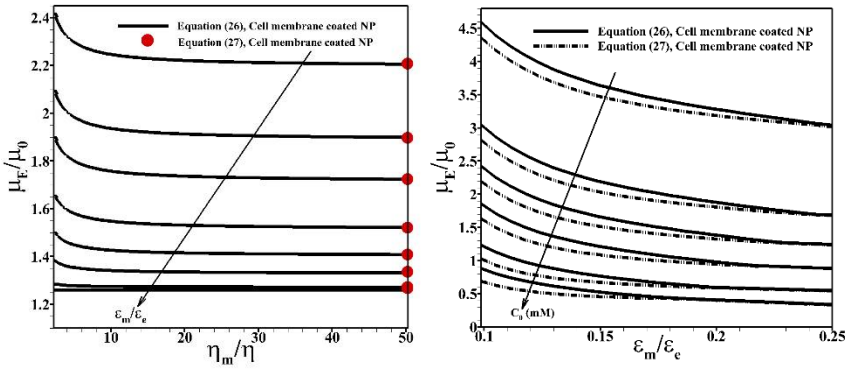

(a) (b)

Figure 4: Variation of scaled electrophoretic mobility μ_E/μ_0 for *cell (biomimetic) membrane-coated NPs* with $\delta = 50$ nm, $\sigma = 2.5 \times 10^{-2}$C/m^2, $N_0 = 10$ mM and $Z = 1$. Results are derived from Eq. (26) and (27) as specified in the figure. Results in panel (a) are shown for the electrophoretic mobility versus the viscosity ratio η_m/η and different dielectric permittivity ratio $\varepsilon_m/\varepsilon_e$=0.09875, 0.1125, 0.125, 0.15, 0.175, 0.2, 0.225, 0.25 at fixed molar concentration of background electrolyte $C_0 = 100$ mM for which $\kappa\delta \gg 1$, with $FC_0 = e\,n_0$. In panel (b), variations of electrophoretic mobility as a function of dielectric permittivity ratio $\varepsilon_m/\varepsilon_e$ for different molar concentrations of background electrolyte C_0 (10, 50, 100, 200, 500, 1000 mM) at fixed viscosity of cell membrane (e.g., $\eta_m = 2.269$ mPa s [147]).

Finally, we give in Figures 4a,b results derived from the mobility expressions (26) and (27) applicable to cell (biomimetic) membrane-coated NPs. The results are indicated in Figure 4a as a function of the viscosity ratio η_m/η for different dielectric permittivity ratios $\varepsilon_m/\varepsilon_e$ and in Figure 4b as a function of the dielectric permittivity ratio $\varepsilon_m/\varepsilon_e$ for different molar concentrations of background electrolyte C_0 with $FC_0 = e\,n_0$. From Figure 4a,b it is clear that the mobility of membrane-coated NPs reduces with increasing the dielectric permittivity ratio $\varepsilon_m/\varepsilon_e$ at fixed ε_e and it approaches a plateau values for $\varepsilon_m/\varepsilon_e > 0.25$. A decrease in $\varepsilon_m/\varepsilon_e$ leads to more significant accumulation of electrolyte ions across the cell membrane layer. As a result, neutralization of membrane charges increases, which leads to a reduction in particle electrophoretic mobility. In addition, particle mobility decreases with increasing electrolyte concentration, in line with enhanced particle charge screening. We further note that particle mobility decreases with increasing viscosity of the membrane layer simply because the frictional force at the membrane-electrolyte interface then increases. At sufficiently high values of the viscosity ratio η_m/η, the particle mobility is correctly predicted by the plateau value given by Eq. (27). We also observe that for cases where the viscosity of the membrane layer is comparable to that of the surrounding aqueous medium, the particle electrophoretic mobility correctly identifies to the Smoluchowski-like expression given by Eq. (27) for $\varepsilon_m/\varepsilon_e \geq 0.25$. Last, the difference between Eqs. (26) and (27) substantially reduces at sufficiently high electrolyte concentrations.

4. Conclusions and perspectives.

This paper reviews progress achieved in the modelling of soft particle DC electrophoresis and it details the various particle types for which such modeling is required so as to retrieve properly their electrostatic properties and, thereby, gain insights into the importance of electrostatics on their stability and, more generally, their reactivity towards neighboring charged (bio)colloids or (bio)surfaces. In particular, the inapplicability of the historical Smoluchowski formulation for particle electrophoretic mobility and underlying zeta potential concept are discussed in relation to the structure of the particles (core-shell, polyelectrolyte, membrane-coated colloids), their defining ion and flow permeability properties as well as their 3D charge distribution. Typical particle systems for which Smoluchowski-based formulation of electrophoretic mobility are inappropriate encompass colloids as diverse as bacterial cells, viral particles, (bio)functionalized (nano)particles, particulate polymeric systems like nanoplastics or environmental particles like humics, fulvics and more generally colloidal organic matter. This review reports useful analytical equations detailing how the electrophoretic mobility depends on key parameters including electrolyte concentration, density of charges distributed across the inner and outer components of the particles, dimensions of particle core and/or shell components when relevant or ratio between dielectric permittivities and viscosities of these components. Future research orientations deal with the corrections of

mean-field electrostatic and/or hydrodynamic formalisms adopted in soft particle electrokinetic modeling so as to include molecular details associated with counterion hydration process, ion polarizability, ion-ion correlation or structure/orientation of interfacial water molecules.

5. CRediT author statement

Gopmandal, Partha P.: Conceptualization, Writing - Original Draft, Visualization.
Duval, Jerome F. L.: Conceptualization, Writing - Original Draft, Visualization.

6. Conflict of interest declaration

The authors declare that they have no competing interests.

7. Acknowledgements

P.P.G. kindly acknowledges the financial support by Science and Engineering Research Board, Govt. of India, through the project grant (File no. MTR/2018/001021).

8. Supporting Information.

Details of the derivation of Eq. (2) given in Table 1.

9. References.

1. Ohshima H. **Theory of colloid and interfacial electric phenomena**. *Elsevier, Academic Press*, vol.12, Amsterdam, 2006.
2. Roth CM. **Encyclopedia of analytical science.** *Electrophoresis*, 2005, 2: 456-460.
3. Maliyah JH, Bhattacharjee S. **Electrokinetic and colloid transport phenomena**. *Wiley-Interscience*, New York, 2006.
4. Schulte A, Chow RH. **A simple method for insulating carbon-fiber microelectrodes using anodic electrophoretic deposition of paint.** *Analytical Chemistry*, 1996, 67:3054–3058.
5. Wong EM, Searson PC. **ZnO quantum particle thin films fabricated by electrophoretic deposition.** *Applied Physics Letters,* 1999, 74:2939–2941.
6. Li J, Gershow M, Stein D, Brandin E, Golovchenko JA. **DNA molecules and configurations in a solid-state nanopore microscope.** *Nature Materials*, 2003, 2:611–615.
7. Wanunu M, Sutin J, Meller A. **DNA profiling using solid-state nanopores: detection of DNA-binding molecules.** *Nano Letters,* 2009, 9:3498–3502.
8. Comiskey B, Albert JD, Yoshizawa H, Jacobson J. **An electrophoretic ink for all-printed reflective electronic displays.** *Nature*, 1998, 394:253–255.
9. Senda K, Usui H. **Fabrication of electrophoretic display driven by membrane switch array.** *Japanese Journal of Applied Physics,* 2010, 49:04DK16.
10. Lyklema J. **Fundamentals of interface and colloid science, vol-II: Solid–liquid interfaces**,

Academic Press, vol.2, New York, 1995.

11. Delgado AV, Gonzalez-Caballero F, Hunter F, Koopal, L, Lyklema J. **Measurement and interpretation of electrokinetic phenomena**. *Journal of Colloid and Interface Science*, 309 (2007): 194-224.

12. Zimmermann R, Duval, JFL, Werner C. **On the analysis of ionic surface conduction to unravel charging processes at macroscopic soft and hard solid-liquid interfaces.** *Current Opinion in Colloid and Interface Science*, 44(2019): 177-187**.**

13. Duval JFL, Wilkinson KJ, Van Leeuwen HP, Buffle J. **Humic substances are soft and permeable: evidence from their electrophoretic mobilities.** *Environmental Science and Technology,* 2005, 39:6435-6445.

14. Hayes MHB, McCarthy P, Malcolm RL, Swift RS. **Humic substances II. In search of structure.** *Wiley Interscience Chichester*, 1989.

15. Klučáková M. **Size and charge evaluation of standard humic and fulvic acids as crucial factors to determine their environmental behavior and impact.** *Front. Chem.*, 2018, 6:235.

16. Smith DE, Dhinojwala A, Moore FBG. **Effect of substrate and bacterial zeta potential on adhesion of mycobacterium smegmatis**. *Langmuir,* 2019, 35, 21: 7035–7042.

17. Sasidharan S, Torkzaban S, Bradford SA, Cook PG, Gupta VVSR. **Temperature dependency of virus and nanoparticle transport and retention in saturated porous media**. *Journal of Contaminant Hydrology*, 196 (2017): 10-20.

18. Loiseau A, Zhang L, Hu D, Salmain M, Mazouzi Y, Flack R, Liedberg B, Boujday S. **Core–shell gold/silver nanoparticles for localized surface plasmon resonance-based naked-eye toxin biosensing.** *ACS Applied Materials & Interfaces*, 2019, 11 (50): 46462-46471

19. Fernández CG, Baños FGD, Esteban MA, Cuesta A. **Functionalized nanoplastics (NPs) increase the toxicity of metals in fish cell lines.** *Int. J. Mol. Sci*, 2021, *22*(13): 7141.

20. Tan J, Jin X, Chen M**. Bio-inspired synthesis of aqueous nanoapatite liquid crystals.** *Scientific Reports*, 2019, 9: 466.

21. Cho WS, Duffin R, Thielbeer F, Bradley M, Megson IL, Macnee W, Poland CA, Tran CA, Donaldson K. **Zeta potential and solubility to toxic ions as mechanisms of lung inflammation caused by metal/metal oxide nanoparticles.** *Toxicol. Sci,* 2012, 126:469-77.

22. Liang X, Liao C, Thompson ML, Soupir ML, Jarboe LR, Dixon PM. **E. coli Surface Properties Differ between Stream Water and Sediment Environments.** *Front. Microbiol.* 2016 7:1732

23. Smoluchowski V. **In handbuch der elektrizitt und des magnetismus; greatz, l., ed.; barth: Leipzig**. *Germany,* 1921, Vol. 2: 366.

24. Hückel E. **The cataphoresis of the sphere.** *Physikalische Zeitschrift,* 1924, 25:204.

25. Henry DC. **The Cataphoresis of Suspended Particles. Part I. The Equation of Cataphoresis**. *Proceedings of the Royal Society of London Series A,* 1931, 133:106-129.

26. Frost R, Langhammer C, Cedervall T. **Real-time in situ analysis of biocorona formation and evolution on silica nanoparticles in defined and complex biological environments**. *Nanoscale,* 2017,9: 3620-3628.

27. * Moussa M, Caillet C, Town RM, Duval JFL. **Remarkable electrokinetic features of charge-stratified soft nanoparticles: mobility reversal in monovalent aqueous electrolyte.** *Langmuir,* 2015, 31:5656-5666.

28. Duval JFL, Farinha JPS. Pinheiro JP. **Impact of electrostatics on the chemodynamics of highly charged metal-polymer nanoparticle complexes.** *Langmuir,* 2013, 29: 13821-13835.

29. ** Duval JFL, Werner C, Zimmermann R. **Electrokinetics of soft polymeric interphases with layered distribution of anionic and cationic charges.** *Current Opinion in Colloid and Interface Science,* 2016, 24: 1-12

30. Revel M, Châtel A, Mouneyrac A. **Micro(nano)plastics: A threat to human health?** *Current Opinion in Environmental Science & Health,* 2018, 1: 17-23

31. Amelia TSM, Khalik WMAWM, Ong MC, Shao YT, Pan HJ, Bhubalan K. **Marine microplastics as vectors of major ocean pollutants and its hazards to the marine ecosystem and humans.** *Progress in Earth and Planetary Science,* 2021, 8: 12.

32. Mattsson K, Hansson LA, Cedervall T. **Nano-plastics in the aquatic environment.** *Environmental Science: Processes and Impacts,* 2015, 17:1712–1721.

33. Shams M, Alam I, Chowdhury I. **Aggregation and stability of nanoscale plastics in aquatic environment**. *Water Research,* 2020, 171:115401.

34. Sharma VK, Ma X, Guo B, Zhang K. **Environmental factors-mediated behavior of microplastics and nanoplastics in water: A review**. *Chemosphere,* 2021, 271:129597.

35. Hartmann NB, Hüffer T, Thompson RC, Hassellöv M, Verschoor A, Daugaard AE, Rist S, Karlsson T, Brennholt N, Cole M, Herrling MP, Hess MC, Ivleva NP, Lusher AL, Wagner M. **Are we speaking the same language? recommendations for a definition and categorization framework for plastic debris.** *Environmental Science and Technology,* 2019, 53:1039-1047.

36. Rios LM, Karapanagioti H, Álvarez NR. **Micro(nanoplastics) in the marine environment: Current knowledge and gaps**. *Current Opinion in Environmental Science & Health,* 2018, 1:47–51.

37. Gigault J, Halle AT, Baudrimont M, Pascal PY, Gauffre F, Phi TL, El Hadri H, Grassl B, Reynaud S. **Current opinion: What is a nanoplastic?** *Environmental Pollution,* 2018, 235:1030-1034.

38. Schwaferts C, Niessner R, Elsner M, Ivleva NP. **Methods for the analysis of submicrometer- and nanoplastic particles in the environment.** *Trends in Analytical Chemistry,* 2019, 112:52-65.

39. Ramirez LR, Gentile SR, Zimmermann S, Stoll, S. **Behavior of TiO2 and CeO2 nanoparticles and polystyrene nanoplastics in bottled mineral, drinking and lake geneva waters. Impact of water hardness and natural organic matter on nanoparticle surface properties and aggregation.** *Water,* 2019, 11:721.

40. Canesi L, Ciacci C, Fabbri R, Balbi T, Salis A, Damonte G, Cortese K, Caratto V, Monopoli MP, Dawson K, Bergami E, Corsi I. **Interactions of cationic polystyrene nanoparticles with marine bivalve hemocytes in a physiological environment: role of soluble hemolymph proteins.** *Environmental Research,* 2016, 150:73–81.

41. Folkersma R, Alois JG, Diemen V, Stein HN. **Electrophoretic properties of polystyrene spheres.** *Langmuir,* 1998, 14(21):5973-5976.

42. Barany S, Nagy M, Skvarla J. **Electrokinetic potential of polystyrene particles in polyelectrolyte and polyelectrolyte mixtures solutions.** *Colloids and Surfaces A: Physicochemical and Engineering Aspects,* 2012, 413:200-207.

43. Hadri HE, Gigault J, Maxit B, Grassl B, Reynaud S. **Nanoplastic from mechanically degraded primary and secondary microplastics for environmental assessments.** *NanoImpact,* 2020, 17:100206.

44. Kobayashi M. **An analysis on electrophoretic mobility of hydrophobic polystyrene particles with low surface charge density: effect of hydrodynamic slip.** *Colloid and Polymer Science,* 2020, 298:1313–1318.

45. Gopmandal PP, Bhattacharyya S, Ohshima H. **On the similarity between the electrophoresis of a liquid drop and a spherical hydrophobic particle.** *Colloid and Polymer Science,* 2017, 295(10):2077–2082.

46. Overbeek JTG. **Polyelectrolytes, past, present and future.** *Pure and Applied Chemistry,* 1976, 46: 91-101.

47. Hsu HP, Lee E. **Counterion condensation of a polyelectrolyte.** *Electrochemistry Communications,* 2012, 15:59-62.

48. Brinkman HC. **A calculation of the viscous force exerted by a flowing fluid on a dense swarm of particles.** *Journal of Applied Sciences Research,* 1947, A1:27-34.

49. Debye P, Bueche AM. **Intrinsic viscosity, diffusion and sedimentation rate of polymers in solution.** The *Journal of Chemical Physics,* 1948, 16:573-579.

50. Heyde ME, Peters CR, Anderson JE. **Factors influencing reverse osmosis rejection of inorganic solutes from aqueous solution.** *Journal of Colloid and Interface Science,* 1975, 50:467-487.

51. ** Hermans JJ, Fujita HK. **Electrophoresis of charged polymer molecules with partial free drainage.** *Proceedings of the Koninklijke Nederlandse Akademie van Wetenschappen. Series B, 1955, 58:182.*

52. Hermans JJ. **Sedimentation and electrophoresis of porous spheres.** *Journal of Polymer Science,* 1955, 18:527-534.

53. Noda I, Nagasawa M, Ota M. **Electrophoresis of a polyelectrolyte in solutions of high ionic strength.** *Journal of the American Chemical Society,* 1964, *86* (23):5075-5079.

54. Hoagland DA, Arvanitidou E, Welch C. **Capillary electrophoresis measurements of the free solution mobility for several model polyelectrolyte systems.** *Macromolecules,* **1999,** *32* (19):6180-6190.

55. Vainshtein P, Shapiro M. **Mobility of permeable fractal agglomerates in slip regime.** *Journal of Colloid and Interface Science,* 2005, 284(2):501-509.

56. Yang Z, Lee DJ, Liu T. **Advective flow of permeable sphere in an electrical field.** *Journal of Colloid and Interface Science,* 2010, 344(1):214-220.

57. Yeh LH, Hsu JP. **Effects of double-layer polarization and counterion condensation on the electrophoresis of polyelectrolytes.** *Soft Matter* 2011 398:396-411.

58. Bhattacharyya S, Gopmandal PP. **Effects of electroosmosis and counterion penetration on electrophoresis of a positively charged spherical permeable particle.** *Soft Matter,* 2013 9:1871-1884.

59. Gopmandal PP, Bhattacharyya S. **Electrokinetics of a charged permeable porous aggregate in an aqueous medium.** *Colloids and Surfaces A: Physicochemical and Engineering Aspects,* 2013, 433:64-76.

60. Langlet J, Gaboriaud F, Gantzer C, Duval JFL. **Impact of chemical and structural anisotropy on the electrophoretic mobility of spherical soft multilayer particles: the case of bacteriophage MS2.** *Biophysical Journal,* 2008, 94:3293–3312.

61. Dika C, Duval JFL, Ly HM, Merlin C, Gantzer C. **Impact of internal RNA on aggregation and electrokinetics of viruses: comparison between MS2 phage and corresponding virus-like particles.** *Applied and Environmental Microbiology,* 2011, 77:4939–4948.

62. ** Sonohara R, Muramatsu N, Ohshima H, Kondo T. **Difference in surface properties between Escherichia coli and Staphylococcus aureus as revealed by electrophoretic mobility measurements.** *Biophysical Chemistry,* 1995, 5:273–277.

63. Bos R, van der Mei HC, Busscher HJ. **'Soft-particle' analysis of the electrophoretic mobility of a fibrillated and non-fibrillated oral streptococcal strain: Streptococcus salivarius.** *Biophysical Chemistry,* 1998, 74:251–255.

64. Duval JFL, Busscher HJ, van de Belt-Gritter B, van der Mei HC, Norde W. **Analysis of the interfacial properties of fibrillated and non-fibrillated oral streptococcal strain from electrophoretic mobility and titration measurements: evidence for the shortcomings of the 'classical soft particle approach'.** *Langmuir,* 2005, 21:11268–11282.

65. ** Duval JFL, Gaboriaud F. **Progress in electrohydrodynamics of soft microbial particle interphases.** *Current Opinion in Colloid and Interface Science,* 2010, 15:184–195.

66. Pagnout C, Présent RM, Billard P, Rotureau E, Duval JFL. **What do luminescent bacterial metal-sensors probe? Insights from confrontation between experiments and flux-based theory.** *Sensors and Actuators B: Chemical,* 2018, 270:482–491.

67. Duval JFL, Pagnout C. **Decoding the time-dependent response of bioluminescent metal-detecting whole-cell bacterial sensors.** *ACS Sensors,* 2019, 4:1373–1383.

68. Merlin J, Duval JFL. **Electrodynamics of soft multilayered particles dispersions: dielectric permittivity and dynamic mobility.** *Physical Chemistry Chemical Physics,* 2014, 16:15173-15188.

69. Martin JRS, Bihannic I, Santos C, Farinha JPS, Demé B, Leermakers FAM, Pinheiro JP, Rotureau E, Duval JFL. **Structure of multiresponsive brush decorated nanoparticles: a combined electrokinetic, DLS, and SANS study.** *Langmuir,* 2015, 31:4779–4790.

70. * Lopez-Viota J, Mandal S, Delgado AV, Toca-Herrera JL, Moller Marco F, Zanuttin M, Krol Balestrino S. **Electrophoretic characterization of gold nanoparticles functionalized with human serum albumin (HSA) and creatine.** *Journal of Colloid and Interface Science,* 2009, 332:215–223.

71. Doane TL, Cheng Y, Babar A, Hill RJ, Burda C. **Electrophoretic mobilities of PEGylated gold NPs.** *Journal of the American Chemical Society,* 2010, 132:15624–15631.

72. Hathout RM, Elshafeey AH. **Development and characterization of colloidal soft nano-carriers for transdermal delivery and bioavailability enhancement of an angiotensin II receptor blocker.** *European Journal of Pharmaceutics and Biopharmaceutics,* 2012, 82:230-240.

73. Ohshima H, Kondo T. **Electrophoresis of large colloidal particles with surface charge layers. Position of the slipping plane and surface layer thickness.** *Colloid and Polymer Science,* 1986, 264:1080–1084.

74. ** Ohshima H, Kondo T. **Electrophoretic mobility and Donnan potential of a large colloidal particle with a surface charge layer.** *Journal of Colloid and Interface Science,* 1987, 116:305–311.

75. Ohshima H, Kondo T. **Approximate analytic expression for the electrophoretic mobility of colloidal particles with surface-charge layers.** *Journal of Colloid and Interface Science,* 1989, 130:281–282.

76. ** Ohshima H, Kondo T. **On the electrophoretic mobility of biological cells.** *Biophysical Chemistry,* 1991, 39:191–198.

77. Zhou F, Huck WTS. **Surface grafted polymer brushes asideal building blocks for ‘‘smart’’ surfaces.** *Physical Chemistry Chemical Physics,* 2006, 8:3815–3823.

78. Ohshima H. **Electrophoretic mobility of soft particle.** *Journal of Colloid and Interface Science,* 1994, 163:474–483.

79. ** Ohshima H. **Electrophoresis of soft particles.** *Advances in Colloid and Interface Science,* 1995, 62:189–235.

80. Ohshima H. **Modified Henry function for the electrophoretic mobility of a charged spherical colloidal particle covered with an ion-penetrable uncharged polymer layer.** *Journal of Colloid and Interface Science,* 2002, 252:119–125.

81. Ohshima H. **Electrophoresis of soft particles: Analytic approximations.** *Electrophoresis,* 2006, 27:526–533.

82. Alexis J. de Kerchove and Menachem Elimelech. **Relevance of electrokinetic theory for "soft" particles to bacterial cells: Implications for bacterial adhesion**. *Langmuir,* 2005, 21: 6462-6472

83. Ohshima H, Makino K, Kato T, Fujimoto K, Kondo T, Kawaguchi H. **Electrophoretic mobility of latex particles covered with temperature-sensitive hydrogel layers.** *Journal of Colloid and Interface Science,* 1993, 159(2):512-514.

84. Nakamura M, Ohshima H, Kondo T. **Electrophoretic behavior of antigen- and antibody-carrying latex particles.** *Journal of Colloid and Interface Science,* 1992, 149:241-246.

85. López-León T, Jódar-Reyes AB, Ortega-Vinuesa JL, Bastos-González D. **Hofmeister effects on the colloidal stability of an IgG-coated polystyrene latex.** *Journal of Colloid and Interface Science,* 2005, 284:139-148.

86. Hayashi H, Tsuneda S, Hirata A, Sasaki H. **Soft particle analysis of bacterial cells and its interpretation of cell adhesion behaviors in terms of DLVO theory.** *Colloids and Surfaces B: Biointerfaces,* 2001, 22:149-157.

87. Morisaki H, Nagai S, Ohshima H, Ikemoto E, Kogure K. **The effect of motility and cell-surface polymers on bacterial attachment.** *Microbiology,* 1999, 145:2797-2802.

88. Takashima S, Morisaki H. **Surface characteristics of the microbial cell of Pseudomonas syringae and its relevance to cell attachment.** *Colloids and Surfaces B: Biointerfaces,* 1997, 9:205-212.

89. * Tsuneda S, Jung J, Hayashi H, Aikawa H, Hirata A, Sasaki H. **Influence of extracellular polymers on electrokinetic properties of heterotrophic bacterial cells examined by soft particle electrophoresis theory.** *Colloids and Surfaces B: Biointerfaces,* 2003, 29:181-188.

90. * Kawahata S, Ohshima H, Muramatsu N, Kondo T. **Charge distribution in the surface region of human erythrocytes as estimated from electrophoretic mobility data.** *Journal of Colloid and Interface Science,* 1990, 138:182-186.

91. Donath E, Budde A, Knippel E, Bäumler H. **"Hairy surface layer" concept of electrophoresis combined with local fixed surface charge density isotherms: Application to human erythrocyte electrophoretic fingerprinting.** *Langmuir,* 1996, 12:4832-4839.

92. Ducel V, Saulnier P, Richard J, Boury F. **Plant protein–polysaccharide interactions in solutions: application of soft particle analysis and light scattering measurements.** *Colloids and Surfaces B: Biointerfaces,* 2005, 41: 95-102.

93. Sakuma S, Ohshima H, Kondo T. **Charge distribution in poly (N,N-l-lysinediylterephthaloyl) microcapsule membranes.** *Journal of Colloid and Interface Science,* 1989, 133:253-256.

94. Nagahama T, Muramatsu N, Ohshima H, Kondo T. **Surface electric characteristics of guinea-pig polymorphonuclear leucocytes.** *Colloids and Surfaces,* 1992, 67:61-65.

95. ** Hill RJ, Saville DA, Russel WB. **Electrophoresis of spherical polymer-coated colloidal particles.** *Journal of Colloid and Interface Science,* 2003, 258(1):56-74.

96. Hill RJ, Saville DA, Russel WB. **Polarizability and complex conductivity of dilute suspensions of spherical colloidal particles with charged (polyelectrolyte) coatings.** *Journal of Colloid and Interface Science,* 2003, 263(2):478-497.

97. Hill RJ, Saville DA. **'Exact' solutions of the full electrokinetic model for soft spherical colloids: Electrophoretic mobility.** *Colloids and Surfaces A: Physicochemical and Engineering Aspects,* 2005, 267:31-49.

98. López-García JJ, Horno J, Grosse C. **Suspended particles surrounded by an inhomogeneously charged permeable membrane. Solution of the Poisson-Boltzmann equation by means of the network method.** *Journal of Colloid and Interface Science,* 2003, 268(2):371-379.

99. Duval JFL, Ohshima H. **Electrophoresis of diffuse soft particles.** *Langmuir,* 2006, 22:3533-3546.

100. Yan Y, Björnmalm M, Caruso F. **Assembly of layer-by-layer particles and their interactions with biological systems**. *Chem. Mater,* 2014, 26(1): 452–460.

101. Ohshima H. **Electrophoretic mobility of soft particles. A soft step function model.** *Colloids and Surfaces A: Physicochemical and Engineering Aspects,* 2014, 440:151-154.

102. Ohshima H. **Electrical phenomena of soft particles. A soft step function model.** *The Journal of Physical Chemistry A,* 2012, 116:6473-6480.

103. Hsu JP, Fan YP. **Electrophoretic mobility of a particle coated with a charged membrane: Effects of fixed charge and dielectric constant distributions.** *Journal of Colloid and Interface Science,* 1995, 172:230-241.

104. Saville DA. **Electrokinetic properties of fuzzy colloidal particles.** *Journal of Colloid and Interface Science,* 2000, 222:137-145.

105. Cametti C. **Dielectric properties of soft-particles in aqueous solutions.** *Soft Matter,* 2011, 7:5494-5506.

106. Hsu HP, Lee E. **Electrophoresis of a single charged porous sphere in an infinite medium of electrolyte solution.** *Journal of Colloid and Interface Science,* 2013, 390:85-95.

107. De S, Bhattacharyya S, Gopmandal PP. **Importance of core electrostatic properties on the electrophoresis of a soft particle.** *Physical Review E,* 2016, 94(2):022611.

108. Bhattacharyya S, De S. **Influence of rigid core permittivity and double layer polarization on the electrophoresis of a soft particle: A numerical study.** *Physics of Fluids,* 2016, 28:012001.

109. Ghoshal UK, Bhattacharyya S, Gopmandal PP, De S. **Nonlinear effects on electrophoresis of a soft particle and sustained solute release.** *Transport in Porous Media,* 2018, 121:121–133.

110. López-García JJ, Horno J, Grosse C. **Suspended particles surrounded by an inhomogeneously charged permeable membrane. Solution of the Poisson-Boltzmann equation by means of the network method.** *Journal of Colloid and Interface Science,* 2003, 268(2):371-379.

111. Ohshima H. **Electrophoretic mobility of a highly charged soft particle: Relaxation effect.** *Colloids and Surfaces A: Physicochemical and Engineering Aspects,* 2011, 376:72-75.

112. Ganjizade A, Ashrafizadeh SN, Sadeghi A. **Effect of ion partitioning on the electrostatics of soft particles with a volumetrically charged core.** *Electrochemistry Communications,* 2017, 84:19-23.

113. Maurya SK, Gopmandal PP, Bhattacharyya S, Ohshima H. **Ion partitioning effect on the electrophoresis of a soft particle with hydrophobic core.** *Physical Review E,* 2018, 98 (2): 023103.

114. Gopmandal PP, De S, Bhattacharyya S, Ohshima H. **Impact of ion-steric and ion-partitioning effects on electrophoresis of soft particles.** *Physical Review E,* 2020, 102(3):032601.

115. Ganjizade A, Ashrafizadeh SN, Sadeghi A. **Effect of ion partitioning on electrophoresis of soft particles.** *Colloid and Polymer Science,* 2019, 297:191-200.

116. Mahapatra P, Gopmandal PP, Duval JFL. **Effects of dielectric gradients-mediated ions partitioning on the electrophoresis of composite soft particles: An analytical theory.** *Electrophoresis,* 2021, 42:153-162.

117. Ashrafizadeh SN, Seifollahi Z, Ganjizade A, Sadeghi A. **Electrophoresis of spherical soft particles in electrolyte solutions: A review.** *Electrophoresis,* 2020, 41(1-2):81-103.

118. Zimmermann R, Dukhin, S.S, Werner C, Duval J.F.L. **On the use of electrokinetics for unraveling charging and structure of soft planar polymer films**. *Current Opinion in Colloid and Interface Science***,** 2013, 18: 83-92.

119. ** Maurya SK, Gopmandal PP, Ohshima H, Duval JFL. **Electrophoresis of composite soft particles with differentiated core and shell permeabilities to ions and fluid flow.** *Journal of Colloid and Interface Science,* 2020, 558:280-290.

120. Rochette CN, Crassous JJ, Drechsler M, Gaboriaud F, De Gaudemaris, Duval JFL. **Shell structure of natural rubber particles: Evidence of chemical stratification by electrokinetics and cryo-TEM.** *Langmuir,* 2013, 29(47):14655-14665.

121. Estelrich J, Quesada-Pérez M, Forcada J, Callejas-Fernández J. **Chapter 1: Introductory aspects of soft nanoparticles**. *In: Callejas-Fernández J, Estelrich J, Quesada-Pérez M, Forcada J, editors. Soft Nanoparticles for Biomedical Applications, Nanoscience & Nanotechnology Series, Royal Society of Chemistry,* 2014, 1-18.

122. Talelli M, Duro-Castaño A, Rodríguez-Escalona G, Vicent MJ. **Smart polymer nanocarriers for drug delivery**. *In: Aguilar MR, Roman JS, editors. Smart Polymers and Their Applications, Woodhead Publishing,* 2014, 327–358.

123. Pepon L, Kenny JM, Navarro-Baena I. **Chapter 13: Shape memory polymers: properties, synthesis and applications.** In: Aguilar MR, Roman JS, editors. *Smart Polymers and Their Applications,* Woodhead Publishing, 2014, 204-236.

124. Masood F. **Polymeric nanoparticles for targeted drug delivery system for cancer therapy**. *Materials Science and Engineering C,* 2016, 60:569–578.

125. Tran S, DeGiovanni PJ, Piel B, Rai P. **Cancer nanomedicine: a review of recent success in drug delivery**. *Clinical and Translational Medicine,* 2017, 6(1):44.

126. Talelli M, Oliveira S, Rijcken CJ, Pieters EH, Etrych T, Ulbrich K, van Nostrum RC, Storm G, Hennink WE, Lammers T. **Intrinsically active nanobody–modified polymeric micelles for tumor-targeted combination therapy**. *Bioma- trials,* 2013, 34(4):1255–1260.

127. Sun T, Zhang YS, Pang B, Hyun DC, Yang M, Xia Y. **Engineered nanoparticles for drug delivery in cancer therapy.** *Angewandte Chemie International Edition,* 2014, 53:2 – 47.

128. Parodi A., Quattrocchi N., van de Ven AL, Chiappini C, Evangelopoulos M, Martinez JO, Brown BS, Khaled SZ, Yazdi IK, Enzo MV, Isenhart L, Ferrari M, Tasciotti E. **Synthetic nanoparticles functionalized with biomimetic leukocyte membranes possess cell-like functions**. *Nature Nanotechnology,* 2012, 8(1):61– 68.

129. Gao C, Lin Z, Wu Z, Lin X, He Q. **Stem cell membrane camouflaging on near-IR photoactivated upconversion nanoarchitectures for in vivo remote-controlled photodynamic therapy.** *Applied Materials & Interfaces,* 2016, 8(50):34252-34260.

130. Fang RH, Hu C-MJ, Luk BT, Gao W, Copp JA, Tai Y, O'Connor DE, Zhang L. **Cancer cell membrane-coated nanoparticles for anticancer vaccination and drug delivery.** *Nano Letters,* 2014, 14(4):2181–2188.

131. Hu C-MJ, Zhang L, Aryal S, Cheung C., Fang RH, Zhang L. **Erythrocyte membrane-camouflaged polymeric nanoparticles as a biomimetic delivery platform**. *Proceedings of the National Academy of Sciences,* 2011, 108(27):10980-10985.

132. Gao C, Lin Z, Jurado-Sánchez B, Lin X, Wu Z, He Q. **Stem cell membrane-coated nanogels for highly efficient in vivo tumor targeted drug delivery**. *Small,* 2016, 12:4056– 4062.

133. Rao L, Bu L-L, Cai B, Xu J-H , Li A, Zhang W-F, Sun Z-J, Guo S-S, Liu W, Wang T-H, and Zhao X-Z. **Cancer cell membrane-coated upconversion nanoprobes for highly specific tumor imaging**. *Advanced Materials,* 2016, 28:3460– 3466.

134. Chen H-Y, Deng J, Wang Y, Wu C-Q, Li X., and Dai H-W. **Hybrid cell membrane-coated nanoparticles: a multifunctional biomimetic platform for cancer diagnosis and therapy**. *ActaBiomaterialia,* 2020, 112:1-13.

135. Patra JK, Das G, Fraceto LF, Campos EVR, Rodriguez-Torres MDP, Acosta-Torres LS, Diaz-Torres LA, Grillo R, Swamy MK, Sharma S, Habtemariam S, Shin HS. **Nano based drug delivery systems: recent developments and future prospects.** *Journal of Nanobiotechnology,* 2018, 16(1):71.

136. Farokhzad OC, Langer R. **Impact of nanotechnology on drug delivery.** *ACS nano,* 2009, 3(1):16-20.

137. Ang CY, Tan SY, Wu S, Tamil SS, ZhaoY. **Synthesis and application of polyacrylic acid-based nanoparticles for photodynamic therapy.** *Official journal of the Controlled Release Society,* 2015, 213:e20-e21.

138. Vijayan V, Uthaman S, Park IK**: Cell membrane-camouflaged nanoparticles: A promising biomimetic strategy for cancer theragnostics.** *Polymers (Basel),* 2018, 10(9):464- 983.

139. Xia Q, Zhang Y, Li Z, Hou X, Feng N. **Red blood cell membrane-camouaged nanoparticles: A novel drug delivery system for antitumor application**. *Acta PharmaceuticaSinica B,* 2019, 9: 675-689.

140. Mauro A, Finkelstein A. **Realistic model of fixed-charge membrane according to the theory of Teorell, Meyer and Sievers.** *The Journal of General Physiology,* 1958, 42: No. 2.

141. Mauro A. **Space charge regions in fixed charge membranes and the associated property of capacitance**. *Biophysical Journal,* 1962, 2: 179-198.

142. Coster HGL. **A quantitative analysis of the voltage-current relationships of fixed charge membranes and the associated property of "punch-through".** *Biophysical Journal,* 1965, 5(5):669–686.

143. Ramírez P. **Donnan equilibrium of ionic drugs in pH-dependent fixed charge membranes: theoretical modeling**. *Journal of Colloid and Interface Science,* 2002, 253(1):171–179.

144. Ohshima H, Nomura K, Kamaya H, Ueda I. **Liquid membrane: Equilibrium potential distribution across lipid monolayer-coated oil/water interface**. *Journal of Colloid and Interface Science,* 1985, 106(2): 470-478.

145. * Jing H, Das S. **Electric double layer electrostatics of lipid-bilayer-encapsulated nanoparticles: Towards a better understanding of protocell electrostatics.** *Electrophoresis,* 2018, 39(5-6): 752-759.

146. Carpenter AP, Foster MJ, Jones KK, Richmond GL. **Effects of salt-induced charge screening on AOT adsorption to the planar and nanoemulsion oil-water interfaces**. *Langmuir,* 2021, doi:10.1021/acs.langmuir.0c01095.

147. ** Mahapatra P, Ohshima H, Gopmandal PP. **Electrophoresis of liquid-layer coated particles: Impact of ion partitioning and ion steric effects**. *Langmuir,* 2021, 37 (38): 11316-11329.

148. Singer SJ, Nicolson GL. **The fluid mosaic model of the structure of cell-membranes.** *Science,*1972, 175: 720-731.

Annotations for references:

[27] * Evidence for sign reversal of electrophoretic mobility of dendrimer particles with varying monovalent electrolyte concentration.

[29] ** Comprehensive review on electrokinetics of soft interfaces featuring chemical heterogeneity.

[51] ** Theoretical (analytical) model for electrophoresis of soft polymeric-like particles.

[62] ** One of the first evidence that electrophoretic response of bacteria reflects their differentiated surface phenotype.

[65] ** Review on electrophoresis of biological cells as tackled beyond the classical hard particle limit.

[70] * Comprehensive electrokinetic characterisation of functionalized gold nanoparticles for biomedical application without invoking inappropriate zeta potential concept.

[74] ** Theoretical (analytical) model for electrophoresis of soft particles in the Donnan electrostatic limit.

[76] ** Theoretical (analytical) model for electrophoresis of soft biological cells.

[79] ** Exhaustive review of the governing set of electrohydrodynamic equations operational in soft particle electrophoresis, and elaboration of analytical expressions in limits of practical interest.

[89] * Comprehensive analysis of surface biopolymers decorating bacteria on the basis of soft surface electrokinetics.

[90] * Application of advanced electrophoresis modelling for adressing electrostatics of erythrocytes.

[95] ** Among the first studies that investigate soft particle electrophoresis from numerical analysis of the complete set of governing electrohydrodynamic equations.

[119] ** Definition of composite soft particles and elaboration of analytical expressions for their electrophoretic mobility in the Debye-Hückel limit.

[145] * Comprehensive description of electrostatics of protocells.

[147] ** Theoretical (analytical) model for the electrophoresis of liquid layer-coated particles applicable to membrane-decorated colloids.

Additional specifications/restrictions of/on electrostatic and hydrodynamic conditions underlying the validity of the reported electrophoretic mobility expressions	**Electrophoretic Mobility Expressions assuming Debye-Hückel approximation (readers are referred to Supporting Information for details)**	**References**	**Equation**
No additional restriction	$\mu_E = \frac{\varepsilon_e \kappa^2}{\eta} C_2 \left[\frac{1}{3}\left(-\frac{2}{\kappa}e^{-\kappa b} + \epsilon_R b E_3(\kappa b) - 3\epsilon_R b E_5(\kappa b)\right) + \frac{2}{3}\frac{L_2}{L_1}\left(\frac{\kappa b+1}{\kappa^2 b}e^{-\kappa b} + \epsilon_R b E_5(\kappa b)\right) + \frac{1}{\lambda_p^2}\left\{\left(\frac{\kappa^2 b^2+\kappa b+1}{\kappa^2 b^3} + \frac{\epsilon_R}{b}\right)e^{-\kappa b} - \frac{2\epsilon_R}{b}E_5(\kappa b)\right\}\right] + \frac{\varepsilon_p}{\eta\lambda_p^2}\frac{C_1(1+\epsilon_R)}{3b^3}[3\kappa_p b\cosh(\kappa_p b) - (3 + \kappa_p^2 b^2)\sinh(\kappa_p b)] - \frac{\varepsilon_p \kappa_p^2}{\eta} C_1 \frac{2(1+p)}{3L_1\lambda^3 b^2}\left[\frac{\kappa_p \lambda_p}{\kappa_p^2-\lambda_p^2}\{\kappa_p b\cosh(\lambda_p b)\sinh(\kappa_p b) - \lambda_p b\cosh(\kappa_p b)\sinh(\lambda_p b)\} + \sinh(\lambda_p b)\sinh(\kappa_p b)\right] + C_2\left(\frac{\varepsilon_p\kappa_p^2-\varepsilon_e\kappa^2}{\eta\lambda_p^2}\right)\frac{1+\epsilon_R}{b}e^{-\kappa b}$	This work	(2)
$\varepsilon_p = \varepsilon_e$	$\mu_E = \frac{\rho_p}{\eta\lambda_p^2}\left[1 + \frac{1}{3}\left(\frac{\lambda_p}{\kappa}\right)^2\left(1 + e^{-2\kappa b} - \frac{1-e^{-2\kappa b}}{\kappa b}\right) + \frac{1}{3}\left(\frac{\lambda_p}{\kappa}\right)^2 \frac{1+\frac{1}{\kappa b}}{\left(\frac{\lambda_p}{\kappa}\right)^2 - 1}\left\{\left(\frac{\lambda_p}{k}\right)\frac{1+e^{-2\kappa b}-\frac{(1-e^{-2\kappa b})}{\kappa b}}{\left(\frac{1+e^{-2\lambda p b}}{1-e^{-2\lambda p b}}\right)-\frac{1}{\lambda_p b}} - (1 - e^{-2\kappa b})\right\}\right]$	Ohshima [78,79]	(3)
$\varepsilon_p = \varepsilon_e, \kappa \to \infty$	$\mu_E = \frac{\rho_p}{\eta\lambda_p^2}$	Ohshima [78]	(4)
$\varepsilon_p = \varepsilon_e,$ $\kappa b \gg 1, \lambda_p b \gg 1$	$\mu_E = \frac{\rho_p}{\eta\lambda_p^2}\left[1 + \frac{2}{3}\left(\frac{\lambda_p}{\kappa}\right)^2\left(\frac{1+\frac{\lambda_p}{2\kappa}}{1+\frac{\lambda_p}{\kappa}}\right)\right]$	Ohshima [78,79], Hermans and Fujita [51]	(5)

$\varepsilon_p = \varepsilon_e, \kappa b \gg 1,$ $\lambda_p \to \infty$	$\mu_E = \frac{1}{3}\frac{\rho_p}{\eta\kappa^2}$	Ohshima [78,79]	(6)

Table 1. Electrophoretic mobility expressions for soft polyelectrolyte particles elaborated under electrohydrodynamic conditions that are specified (left column). The mathematical model and detailed derivation of the original mobility expression reported in this Table (Eq. (2)) are provided in **Supporting Information**. The constants C_1, C_2, L_1, L_2 and ϵ_R involved in the mobility expressions collected in **Table 1** are defined below:

$C_1 = -\frac{b\varepsilon_e(\kappa b+1)\rho_p}{\varepsilon_P\kappa_p^2[b\kappa_p\varepsilon_p\cosh(\kappa_p b)+(-\varepsilon_P+\varepsilon_e(\kappa b+1))\sinh(\kappa_p b)]}$, $C_2 = \frac{be^{\kappa b}\rho_p[\kappa_p b\cosh(\kappa_p b)-\sinh(\kappa_p b)]}{\kappa_p^2[b\kappa_p\varepsilon_p\cosh(\kappa_p b)+(-\varepsilon_p+\varepsilon_e(\kappa b+1))\sinh(\kappa_p b)]}$, $L_1 = \cosh(\lambda_p b) - \frac{\sinh(\lambda_p b)}{\lambda_p b}$, $L_2 = \cosh(\lambda_p b)$ and $\epsilon_R = \frac{(\varepsilon_e/\varepsilon_p)-1}{(2\varepsilon_e/\varepsilon_p)+1}$.

Additional specifications/restrictions of/on electrostatic and hydrodynamic conditions underlying the validity of the reported electrophoretic mobility expressions	Electrophoretic Mobility Expressions based on flat-plate representation of core-shell composite (nano)particles within Debye-Hückel approximation	Refe-rences	Equa-tion
Composite nanoparticles with soft core-soft shell (Sc-Ssl)			
No additional restriction	$$\mu_E = \frac{\varepsilon_e \psi_{DON}}{\eta}\left[\frac{\varepsilon_c F_2}{\varepsilon_e F_1}\left([1-\cosh(\kappa_{sl}d)] + P\left\{\cosh(\kappa_{sl}d) + \frac{\varepsilon_e}{\varepsilon_{sl}}\frac{\kappa}{\kappa_{sl}}\sinh(\kappa_{sl}d)\right\}\right)\right.$$ $$+\frac{\varepsilon_{sl}}{\varepsilon_e}\frac{1}{F_1}\left([\cosh(\lambda_{sl}d)-1] + (P-1)\frac{\lambda_{sl}^2}{\lambda_{sl}^2-\kappa_{sl}^2}\{\cosh(\lambda_{sl}d)-\cosh(\kappa_{sl}d)\}\right.$$ $$-\frac{\varepsilon_e}{\varepsilon_{sl}}\frac{k}{k_{sl}}P\frac{\lambda_{sl}^2}{\lambda_{sl}^2-\kappa_{sl}^2}\left\{\sinh(k_{sl}d)-\frac{k_{sl}}{\lambda_{sl}}\sinh(\lambda_{sl}d)\right\}$$ $$+\frac{\lambda_{sl}}{\lambda_c}\coth\left(\frac{\lambda_c L}{2}\right)\left\{\sinh(\lambda_{sl}d) + (P-1)\frac{\lambda_{sl}^2}{\lambda_{sl}^2-\kappa_{sl}^2}\left(\sinh(\lambda_{sl}d)-\frac{\kappa_{sl}}{\lambda_{sl}}\sinh(\kappa_{sl}d)\right)\right.$$ $$\left.\left.-\frac{\varepsilon_e}{\varepsilon_{sl}}\frac{\kappa\lambda_{sl}}{\lambda_{sl}^2-\kappa_{sl}^2}P(\cosh(\kappa_{sl}d)-\cosh(\lambda_{sl}d))\right\}\right) + \frac{\varepsilon_{sl}}{\varepsilon_e}\left(\frac{\kappa_s l}{\lambda_{sl}}\right)^2\left(1-\frac{1}{F_1}\right)$$ $$\left.+\left(\frac{\varepsilon_s l}{\varepsilon_e}-\frac{\varepsilon_c}{\varepsilon_e}\right)\frac{1}{F_1}\left([1-\cosh(\kappa_{sl}d)] + P\left\{\cosh(\kappa_{sl}d) + \frac{\varepsilon_e}{\varepsilon_{sl}}\frac{\kappa}{\kappa_{sl}}\sinh(\kappa_{sl}d)\right\}\right) + P\left(1-\frac{\varepsilon_{sl}}{\varepsilon_e}\right)\right]$$ $$+\frac{\rho_{core}}{\eta\kappa_c^2}\left[\frac{\varepsilon_c}{\varepsilon_e}\frac{F_2}{F_1}Q\left(\cosh(\kappa_{sl}d) + \frac{\varepsilon_e}{\varepsilon_{sl}}\frac{\kappa}{\kappa_{sl}}\sinh(\kappa_{sl}d)\right) + \left(\frac{1-F_2}{F_1}\right)\right.$$ $$+\frac{\varepsilon_{sl}}{\varepsilon_e}\frac{1}{F_1}Q\left\{\frac{\lambda_{sl}^2}{\lambda_{sl}^2-\kappa_{sl}^2}\{\cosh(\lambda_{sl}d)-\cosh(\kappa_{sl}d)\} - \frac{\varepsilon_e}{\varepsilon_{sl}}\frac{k}{k_{sl}}\frac{\lambda_{sl}^2}{\lambda_{sl}^2-\kappa_{sl}^2}\left(\sinh(k_{sl}d)-\frac{k_{sl}}{\lambda_{sl}}\sinh(\lambda_{sl}d)\right)\right.$$ $$\left.\left.+\frac{\lambda_{sl}}{\lambda_c}\coth\left(\frac{\lambda_c L}{2}\right)\left(\frac{\lambda_{sl}^2}{\lambda_{sl}^2-\kappa_{sl}^2}\left(\sinh(\lambda_{sl}d)-\frac{\kappa_{sl}}{\lambda_{sl}}\sinh(\kappa_{sl}d)\right) - \frac{\varepsilon_e}{\varepsilon_{sl}}\frac{\kappa\lambda_{sl}}{\lambda_{sl}^2-\kappa_{sl}^2}(\cosh(\kappa_{sl}d)-\cosh(\lambda_{sl}d))\right)\right\}$$ $$\left.+\frac{\kappa_c^2}{\lambda_c^2}\frac{1}{F_1} + \left(\frac{\varepsilon_{sl}}{\varepsilon_e}-\frac{\varepsilon_c}{\varepsilon_e}\right)\frac{1}{F_1}Q\left(\cosh(\kappa_{sl}d) + \frac{\varepsilon_e}{\varepsilon_{sl}}\frac{\kappa}{\kappa_{sl}}\sinh(\kappa_{sl}d)\right) + Q\left(1-\frac{\varepsilon_{sl}}{\varepsilon_e}\right)\right]$$	Mahapatra et al. [116]	(8)
$\kappa>>1$, $\kappa_c>>1$ and $\kappa_{sl}>>1$	$$\mu_E = \frac{\rho_{shell}}{\eta\lambda_{sl}^2}\left(1-\frac{1}{F_1}\right) + \frac{\rho_{core}}{\eta\lambda_c^2}\frac{1}{F_1}$$	Mahapatra et al. [116]	(9)
$\lambda_c L \gg 1, \lambda_{sl}d \gg 1$, $\kappa_c L \gg 1, \kappa_{sl}d \gg 1$	$$\mu_E = \frac{\varepsilon_{sl}}{\eta}\left(\frac{\frac{\psi_{DON}}{\lambda_{sl}}+\frac{\psi(0)}{\kappa_{sl}}}{\frac{1}{\kappa_{sl}}+\frac{1}{\lambda_{sl}}}\right) + \frac{\rho_{shell}}{\eta\lambda_{sl}^2} + \frac{1}{\eta}(\varepsilon_e-\varepsilon_{sl})\psi(0) \text{ with } \psi(0) = \psi_{DON}/\left(1+\frac{\varepsilon_e}{\varepsilon_{sl}}\frac{\kappa}{\kappa_{sl}}\right)$$	Mahapatra et al. [116]	(10)

$\lambda_c L \gg 1, \lambda_{sl} d \gg 1$, $\kappa_c L \gg 1, \kappa_{sl} d \gg 1$ and $\varepsilon_{sl} = \varepsilon_e$	$\mu_E = \frac{\varepsilon_e}{\eta}\left(\frac{\frac{\psi_{DON}}{\lambda_{sl}}+\frac{\psi(0)}{\kappa_{sl}}}{\frac{1}{\kappa_{sl}}+\frac{1}{\lambda_{sl}}}\right) + \frac{\rho_{shell}}{\eta\lambda_{sl}^2}$ with $\psi(0) = \psi_{DON}/2$	Ohshima [78,79]	(11)
$\lambda_c L \gg 1, \lambda_{sl} d \gg 1$, $\kappa_c L \gg 1, \kappa_{sl} d \gg 1$, $\varepsilon_{sl} = \varepsilon_e$ and $\lambda_{sl} \to \infty$	$\mu_E = \frac{\varepsilon_e}{\eta}\psi(0)$ with $\psi(0) = \psi_{DON}/2$	Smoluchowski [23]	(12)
Composite nanoparticles with semisoft core-soft shell (SSc-Ssl)			
No additional restriction	$\mu_E = \frac{\varepsilon_{sl}}{\eta}\psi_{DON}\left[\frac{\kappa_{sl}^2}{\kappa_{sl}^2-\lambda_{sl}^2}\left(1-\frac{\cosh(\kappa_{sl}d)}{\cosh(\lambda_{sl}d)}\right) + P\frac{\kappa_{sl}^2}{\kappa_{sl}^2-\lambda_{sl}^2}\frac{1}{\cosh(\lambda_{sl}d)}\left\{\cosh(\kappa_{sl}d) + \frac{\varepsilon_e}{\varepsilon_{sl}}\frac{\kappa}{\kappa_{sl}}\sinh(\kappa_{sl}d)\right\} + P\frac{\lambda_{sl}^2}{\lambda_{sl}^2-\kappa_{sl}^2}\left\{1 + \frac{\varepsilon_e}{\varepsilon_{sl}}\frac{\kappa}{\lambda_{sl}}\tanh(\lambda_{sl}d)\right\} + \left(\frac{\kappa_{sl}}{\lambda_{sl}}\right)^2\left\{1-\frac{1}{\cosh(\lambda_{sl}d)}\right\} + \left(\frac{\varepsilon_e}{\varepsilon_{sl}}-1\right)P\right] + \frac{\varepsilon_{sl}}{\varepsilon_e}\frac{\rho_{core}}{\eta\kappa_c^2}Q\left[\frac{\kappa_{sl}^2}{\kappa_{sl}^2-\lambda_{sl}^2}\frac{1}{\cosh(\lambda_{sl}d)}\left\{\cosh(\kappa_{sl}d) + \frac{\varepsilon_e}{\varepsilon_{sl}}\frac{\kappa}{\kappa_{sl}}\sinh(\kappa_{sl}d)\right\} + \frac{\lambda_{sl}^2}{\lambda_{sl}^2-\kappa_{sl}^2}\left\{1 + \frac{\varepsilon_e}{\varepsilon_{sl}}\frac{\kappa}{\lambda_{sl}}\tanh(\lambda_{sl}d)\right\} + \left(\frac{\varepsilon_e}{\varepsilon_{sl}}-1\right)\right]$	Mahapatra et al. [116]	(13)
Composite nanoparticles with semisoft core-semisoft shell (SSc-SSsl)			
No additional restriction	$\mu_E = \frac{\varepsilon_e}{\eta}\left(\psi_{DON}\,P + \frac{\rho_{core}}{\varepsilon_e\kappa_c^2}\,Q\right)$	Mahapatra et al. [116]	(14)
Composite nanoparticles with Hard core-soft shell (Hard core-Ssl)			
No additional restriction	$\mu_E = \frac{\varepsilon_{sl}}{\eta}\psi_{DON}\left[\frac{\kappa_{sl}^2}{\kappa_{sl}^2-\lambda_{sl}^2}\left(1-\frac{\cosh(\kappa_{sl}d)}{\cosh(\lambda_{sl}d)}\right) + R\frac{\lambda_{sl}^2}{\lambda_{sl}^2-\kappa_{sl}^2}\left\{1 + \frac{\varepsilon_e}{\varepsilon_{sl}}\frac{\kappa}{\lambda_{sl}}\tanh(\lambda_{sl}d)\right\} + R\frac{\kappa_{sl}^2}{\kappa_{sl}^2-\lambda_{sl}^2}\frac{1}{\cosh(\lambda_{sl}d)}\left\{\cosh(\kappa_{sl}d) + \frac{\varepsilon_e}{\varepsilon_{sl}}\frac{\kappa}{\kappa_{sl}}\sinh(\kappa_{sl}d)\right\} + \left(\frac{\kappa_{sl}}{\lambda_{sl}}\right)^2\left(1-\frac{1}{\cosh(\lambda_{sl}d)}\right) + (\frac{\varepsilon_e}{\varepsilon_{sl}}-1)R\right] + \frac{\rho_{core}L}{2\eta\kappa_{sl}}\left[S\frac{\kappa_{sl}^2}{\kappa_{sl}^2-\lambda_{sl}^2}\frac{1}{\cosh(\lambda_{sl}d)}\left(\cosh(\kappa_{sl}d) + \frac{\varepsilon_e}{\varepsilon_{sl}}\frac{\kappa}{\kappa_{sl}}\sinh(\kappa_{sl}d)\right) + S\frac{\lambda_{sl}^2}{\lambda_{sl}^2-\kappa_{sl}^2}\left(1 + \frac{\cosh(\lambda_{sl}d)\,\varepsilon_e}{\varepsilon_{sl}}\frac{\kappa}{\lambda_{sl}}\tanh(\lambda_{sl}d)\right) + \left(\frac{\varepsilon_e}{\varepsilon_{sl}}-1\right)S\right]$	Mahapatra et al. [116]	(15)
$\lambda_{sl} d \gg 1, \kappa_{sl} d \gg 1 \varepsilon_{sl} = \varepsilon_e, \rho_{core} = 0$	$\mu_E = \frac{\rho_{shell}}{\eta\lambda_{sl}^2}\left(1 + \frac{2}{3}\left(\frac{\lambda_{sl}}{\kappa}\right)^2\frac{1+\lambda_{sl}/2\kappa}{1+\lambda_{sl}/\kappa}\left\{1 + \frac{1}{2(1+2d/L)}\right\}\right)$	Ohshima [79]	(16)

$\lambda_{sl}d \gg 1, \kappa_{sl}d \gg 1$ $\varepsilon_{sl} = \varepsilon_e, \rho_{core} = 0$ and $L/2 \gg d$	$\mu_E = \frac{\rho_{shell}}{\eta\lambda_{sl}^2}\left(1 + \left(\frac{\lambda_{sl}}{\kappa}\right)^2 \frac{1 + \lambda_{sl}/2\kappa}{1 + \lambda_{sl}/\kappa}\right)$	Ohshima [79]	(17)
$\lambda_{sl} \to \infty, \kappa_{sl}d \gg 1$ $\varepsilon_{sl} = \varepsilon_e, \rho_{core} = 0$ and $L/2 \gg d$	$\mu_E = \frac{\varepsilon_e}{\eta}\psi(0)$ with $\psi(0) = \psi_{DON}/2$	Ohshima [79]	(18)
$\lambda_{sl}d \gg 1, \kappa_{sl}d \gg 1$ $\varepsilon_{sl} = \varepsilon_e, \rho_{core} = 0$ and $L/2 \ll d$	$\mu_E = \frac{\rho_{shell}}{\eta\lambda_{sl}^2}\left(1 + \frac{2}{3}\left(\frac{\lambda_{sl}}{\kappa}\right)^2 \frac{1 + \lambda_{sl}/2\kappa}{1 + \lambda_{sl}/\kappa}\right)$	Ohshima [78,79] Hermans and Fujita [51]	(19)
$\lambda_{sl} \to \infty, , \kappa_{sl}d \gg 1$ $\varepsilon_{sl} = \varepsilon_e, \rho_{core} = 0$ and $L/2 \ll d$	$\mu_E = \frac{2}{3}\frac{\varepsilon_e}{\eta}\psi(0)$ with $\psi(0) = \psi_{DON}/2$	Ohshima [78]	(20)
$\varepsilon_{sl} = \varepsilon_e$ with $L \to 0$ and $\rho_{core} \to \infty$ with the product $L \times \rho_{core}/2 \to \sigma$ (here σ is the surface charge density of the core	$\mu_E = \frac{\sigma}{\eta\kappa}\left[\frac{\kappa^2}{\kappa^2 - \lambda_{sl}^2}\frac{1}{\cosh(\lambda_{sl}d)} - \frac{\lambda_{sl}^2}{\kappa^2 - \lambda_{sl}^2}e^{-\kappa d}\left(1 + \frac{\kappa}{\lambda_{sl}}\tanh(\lambda_{sl}d)\right)\right]$	Ohshima [79]	(21)
Composite nanoparticles with Hard core-semisoft shell (Hard core-SSsl)			
No additional restriction	$\mu_E = \psi_{DON}\frac{\varepsilon_e}{\eta}R + \frac{\rho_{core}L}{2\eta\kappa_{sl}}\frac{\varepsilon_e}{\varepsilon_{sl}}S$	Mahapatra et al. [116]	(22)

Table 2. Summary of several closed form analytical expressions for the electrophoretic mobility of several composite core-shell soft particles specified in the main text. Here κ^{-1} is the EDL thickness defined by $\kappa^{-1} = \sqrt{\varepsilon_e k_B T/2e^2 z^2 n_0}$ and the parameters κ_c and κ_{sl} are defined by $\kappa_c^2 = f_c\kappa^2\varepsilon_e/\varepsilon_c$ and $\kappa_{sl}^2 = f_{sl}\kappa^2\varepsilon_e/\varepsilon_{sl}$, respectively. Here f_c and f_{sl} are ion partitioning coefficients of the mobile electrolyte ions within the core and shell compartments, respectively. A detailed description of the ion partitioning coefficients are described in the main text. The Donnan potential ψ_{DON} and potential $\psi(0)$ at the interface between the outer shell layer and electrolyte solution are defined as $\psi_{DON} = \frac{\rho_{shell}}{\varepsilon_{sl}\kappa_{sl}^2}$ and $\psi(0) = \psi_{DON}P + Q\frac{\rho_{core}}{\varepsilon_e\kappa_c^2}$. The various parameters involved in the mobility expressions provided in **Table 2** are given below

$$
\begin{cases}
P = \dfrac{\kappa_{sl}\dfrac{\varepsilon_{sl}}{\varepsilon_e}\sinh(\kappa_{sl}d) - \kappa_c\dfrac{\varepsilon_c}{\varepsilon_e}\{1-\cosh(\kappa_{sl}d)\}\tanh\left(\dfrac{\kappa_c L}{2}\right)}{\left[\kappa_c\dfrac{\varepsilon_c}{\varepsilon_e}\left\{\cosh(\kappa_{sl}d) + \dfrac{\varepsilon_e}{\varepsilon_{sl}}\dfrac{\kappa}{\kappa_{sl}}\sinh(\kappa_{sl}d)\right\}\tanh\left(\dfrac{\kappa_c L}{2}\right)\right] + \left[\kappa_{sl}\dfrac{\varepsilon_{sl}}{\varepsilon_e}\left\{\sinh(\kappa_{sl}d) + \dfrac{\varepsilon_e}{\varepsilon_{sl}}\dfrac{\kappa}{\kappa_{sl}}\cosh(\kappa_{sl}d)\right\}\right]} \\
Q = \dfrac{\kappa_c\tanh\left(\dfrac{\kappa_c L}{2}\right)}{\left[\kappa_c\dfrac{\varepsilon_c}{\varepsilon_e}\left\{\cosh(\kappa_{sl}d) + \dfrac{\varepsilon_e}{\varepsilon_{sl}}\dfrac{\kappa}{\kappa_{sl}}\sinh(\kappa_{sl}d)\right\}\tanh\left(\dfrac{\kappa_c L}{2}\right)\right] + \left[\kappa_{sl}\dfrac{\varepsilon_{sl}}{\varepsilon_e}\left\{\sinh(\kappa_{sl}d) + \dfrac{\varepsilon_e}{\varepsilon_{sl}}\dfrac{\kappa}{\kappa_{sl}}\cosh(\kappa_{sl}d)\right\}\right]} \\
R = \dfrac{\sinh(\kappa_{sl}d)}{\sinh(\kappa_{sl}d) + \dfrac{\varepsilon_e}{\varepsilon_{sl}}\dfrac{\kappa}{\kappa_{sl}}\cosh(\kappa_{sl}d)} \\
S = \dfrac{1}{\sinh(\kappa_{sl}d) + \dfrac{\varepsilon_e}{\varepsilon_{sl}}\dfrac{\kappa}{\kappa_{sl}}\cosh(\kappa_{sl}d)} \\
F_1 = \cosh(\lambda_{sl}d) + \left(\dfrac{\lambda_{sl}}{\lambda_c}\right)\coth\left(\dfrac{\lambda_c L}{2}\right)\sinh(\lambda_{sl}d) \\
F_2 = \dfrac{1 - \left(\dfrac{\kappa_c}{\lambda_c}\right)\coth\left(\dfrac{\lambda_c L}{2}\right)\tanh\left(\dfrac{k_c L}{2}\right)}{1 - \dfrac{\kappa_c^2}{\lambda_c^2}}
\end{cases}
$$

Particle type	**Additional conditions** (other than the conditions of (i) a particle size that well exceeds the EDL thickness and (ii) a low to moderate particle charge) underlying the validity of the reported electrophoretic mobility expressions	**Electrophoretic Mobility Expressions**	**Equation**
Sc-Ssl NPs	$\lambda_c L \gg 1, \lambda_{sl} d \gg 1,$ $\kappa_c L \gg 1, \kappa_{sl} d \gg 1$ and $\lambda_{sl} \to \infty$	$\mu_E = \frac{\varepsilon_e \psi(0)}{\eta}$ with $\psi(0) = \psi_{DON}/2$ and $\psi_{DON} = \frac{\rho_{shell}}{\varepsilon_e \kappa^2}$	(28)
SSc-SSsl NPs	No additional restriction	$\mu_E = \frac{\varepsilon_e \psi(0)}{\eta}$ with $\psi(0) = \left(\psi_{DON}\, P + \frac{\rho_{core}}{\varepsilon_e \kappa_c^2}\, Q\right)$	(29)
	$\kappa_c L \gg 1, \kappa_{sl} d \gg 1$ and $\kappa d \gg 1$	$\mu_E = \frac{\varepsilon_e \psi(0)}{\eta}$ with $\psi(0) = \psi_{DON}/(1 + \frac{\kappa \varepsilon_e}{\kappa_{sl} \varepsilon_{sl}})$ and $\psi_{DON} = \frac{\rho_{shell}}{\varepsilon_e \kappa^2}$	(30)
	$\kappa_c L \gg 1, \kappa_{sl} d \gg 1, \kappa d \gg 1$ and $\varepsilon_{sl} = \varepsilon_e$	$\mu_E = \frac{\varepsilon_e \psi(0)}{\eta}$ with $\psi(0) = \psi_{DON}/2$ and $\psi_{DON} = \frac{\rho_{shell}}{\varepsilon_e \kappa^2}$	(31)
Hard Core-Ssl NPs	$\lambda_{sl} \to \infty, \kappa_{sl} d \gg 1$ $\varepsilon_{sl} = \varepsilon_e, \rho_{core} = 0$ and $L/2 \gg d$	$\mu_E = \frac{\varepsilon_e}{\eta} \psi(0)$ with $\psi(0) = \psi_{DON}/2$	(32)
	$\lambda_{sl} \to \infty, , \kappa_{sl} d \gg 1$ $\varepsilon_{sl} = \varepsilon_e, \rho_{core} = 0$ and $L/2 \ll d$	$\mu_E = \frac{2}{3} \frac{\varepsilon_e}{\eta} \psi(0)$ with $\psi(0) = \psi_{DON}/2$	(33)
Hard Core- SSsl NPs	No additional restriction	$\mu_E = \frac{\varepsilon_e \psi(0)}{\eta}$ with $\psi(0) = \psi_{DON} R + \frac{\rho_{core} L}{2\eta \varepsilon_{sl} \kappa_{sl}} S$ and $\psi_{DON} = \frac{\rho_{shell}}{\varepsilon_e \kappa^2}$	(34)
	$\kappa_{sl} d \gg 1$	$\mu_E = \frac{\varepsilon_e \psi(0)}{\eta}$ with $\psi(0) = \psi_{DON}/(1 + \frac{\kappa \varepsilon_e}{\kappa_{sl} \varepsilon_{sl}})$ and $\psi_{DON} = \frac{\rho_{shell}}{\varepsilon_e \kappa^2}$	(35)
	$\kappa_{sl} d \gg 1$and $\varepsilon_{sl} = \varepsilon_e$	$\mu_E = \frac{\varepsilon_e \psi(0)}{\eta}$ with $\psi(0) = \psi_{DON}/2$ and $\psi_{DON} = \frac{\rho_{shell}}{\varepsilon_e \kappa^2}$	(36)

Cell membrane coated core-shell NPs	$\eta_m \gg \eta$	$\mu_E = \frac{\varepsilon_e \psi(0)}{\mu_e}$, with $\psi(0) = \frac{\frac{\sigma}{\varepsilon_e k} - Sgn(\psi(0))\psi_{DON}\sqrt{f_m \frac{\varepsilon_m}{\varepsilon_e}(1+Zy_{DON})}}{1 - Sgn(\psi(0))\sqrt{f_m \frac{\varepsilon_m}{\varepsilon_e}(1+Zy_{DON})}}$ and $\psi_{DON} = \frac{k_B T}{ze}\left[\frac{ZN_0}{2zf_m n_0} + \sqrt{1 + \left(\frac{ZN_0}{2zf_m n_0}\right)^2}\right]$ and $y_{DON} = e\psi_{DON}/k_B T$	(37)

Table 3. Summary of several Smoluchowski-like mobility expressions for several core-shell composite NPs specified in the main text. Symbol Notation are specified in the main text and Figure captions.

Highlights (85 characters per bullet point)

- Physical reasons for limits of zeta potential concept are provided for soft interfaces
- Expressions for the electrophoretic mobility of soft polyelectrolytes are given
- Expressions for the electrophoretic mobility of core-shell particles are given
- Expressions for the electrophoretic mobility of membrane-coated particles are given
- Effects of dielectric decrements on particle electrophoresis are discussed
- Illustrations of some key features of soft particle electrokinetic response

Electrostatics and electrophoresis of engineered nanoparticles and particulate environmental contaminants : beyond zeta potential-based formulation.

Partha P. Gopmandal,[a] Jérôme F. L. Duval,[b] *

[a] Department of Mathematics, National Institute of Technology Durgapur, Durgapur-713209, India.

[b] Université de Lorraine, CNRS, Laboratoire Interdisciplinaire des Environnements Continentaux (LIEC), UMR 7360 CNRS-Université de Lorraine, Vandoeuvre-lès-Nancy F-54501, France.

*Corresponding Author: Jérôme F. L. Duval. Email: jerome.duval@univ-lorraine.fr

Graphical Abstract.